FULL REPORTS

Report Editor: Erhan COŞKUN

Department of Mathematics,

Karadeniz Technical University, Trabzon, 2011

http://matendustri.ktu.edu.tr

Preface v
Acknowledgements vii
Adaptive Light Control System viii
1. Model 10
2. Continuous traffic model 12
3. Conclusions 15
4. Recommendations 15
5. Acknowledgements 15
6. References 16
Spinning Soccer Ball Trajectory 17
Abstract 19
1. Statement of the problem 19
2. Introduction and background 20
3. Observations 23
4. The proposed model 24
5. Results: Trajectory of the ball 25
6. Discussion 27
Acknowledgments 29
References 29
Handgun Accuracy Problem 32
1.A handgun problem 34
2. Introduction 34
3. Gun Specification 35
4. Problem Approach 36
5. Analysis 38
5.1 Heating 38
5.2 Recoil spring motion 39
5.3 Vice motion. 39
5.4 Barrel assembly motion during firing 40
6. Rifling 41
7. Conclusions 43
8. Acknowledgements 43
References 43
A Medical Waste Sterilizer 44
1. Problem Statement 46
2. Models and analysis 48
3. Optimal Rotational Velocity 53
4. Conclusions and recommendations 55
5. Acknowledgements 55
References 56
Participants 57

Executive Committee

Organizer	Erhan COŞKUN
Web	Ahmet GÖKDOĞAN
Financing	Zafer ÇAKIR
	Ayşe KABATAŞ Elif BAŞKAYA
Housing	Selçuk Han AYDIN
	Tülay KESEMEN
	Olgun CABRİ
Social Activities	Mehmet MERDAN
	İshak CUMHUR
	Süleyman ŞENGÜL
	Devran YAZIR

Ömer AKIN, TOBB ETU

Bülent KARASÖZEN, METU

Invited Participants

John OCKENDON, Oxford University
OCCAM

Ellis Cumberbatch(Claremont Graduate School, USA)

Tim Reiss(Oxford)

W. Chen(Oxford)

K. Bentahar(Oxford)

Dr. George Türkiyyah(American Univ. Lb)

Advisory Board

Adnan BAKİ	Alemdar Bayraktar(KTÜ Faculty of Engineering) İsmail H. ALTAŞ
Mustafa BAYRAM, YTU	Temel KAYIKÇIOĞLU
Haskız COŞKUN	İsmail KAYA
Abdullah ÇAVUŞ	İbrahim OKUMUŞ
Cevat HACIYEV	Vasıf NABİYEV
Zameddin İSMAİLOV	Murat EKİNCİ
Dr.Tahir KHANIEV, TOBB, ETU	Cemal KÖSE
ÖMER PEKŞEN	Mustafa ULUTAŞ
Münevver TEZER, ODTÜ	Alican DALOĞLU
İhsan ÜNVER	Hasan SOFUOĞLU
Ziya YAPAR	Ahmet ÜNAL
Yüksel VARDAR, TOBB	Mete AVCI

Preface

1st Euro-Asian Study Group, 04-08 October, 2010 Trabzon, Turkey

Study groups, initiated originally by a group of researchers at Oxford University, are held regularly around the world with the aim of developing new mathematical models, or enhancing the existing ones to better suit the needs of industry. To this end, groups of academics, who feel confident in applying mathematics to real-world problems, and industry representatives get together and work on problems posed by the firms during a week; this week is announced usually at the so-called international study group website(www.maths-in-industry.org).

Such a collaborative work usually begins in Monday morning with problem presentations by the firm members to an audience of mostly applied mathematians, followed by study groups formed around problems of relevant interest. People feel free to chose the problem they would like to work on, but are not required to stick with the problem they have begun with.

Study groups attract people of diverse interests and backgrounds around a problem and provide in return many benefits to the participants:

> The firm representatives have at least a better clue for the solution of their problem, if not the partial or better solution. This will give the opportunity for future collaboration and expectation for mutual benefit.
>
> The senior academics who feel the heaviest burden find themselves often in a state to seek help from the young researchers of relevant subjects, thus enabling a frank but cordial discussion environment far from the rank-associated barriers that often exist in academic environments. The winners in this environment are surely the young researchers, who attack a problem posed by a firm; this itself is a major step in their otherwise theoretically-oriented reseach path. What can make a young researcher happier in the world of mathematics than the ideas that receive credit from their senior masters!
>
> I guess the triumph of study groups lies in the humble discussion environment created by the senior members of the study groups just before the beginning of the discussion groups. Who feels to be ashamed of producing a stupid idea or an answer while they all are generously being classified under the so-called "colemanballs"? (http://people.maths.ox.ac.uk/~howison/balls.pdf) Who would be affaid of expressing his/her ideas when someone says "Give me an idea(or say a parameter), I do not care what it is, I will use it." Maybe this style could be extended down (or up) to our regular lecture rooms or classrooms as well. Wouldn't this allow for a better learning "room" than is traditional?
>
> On the other hand, Study groups are places that you always remind you of the saying that there is no such thing as a free meal. Get around in a warm place with people of varying fames and abilities in a rather humble discussion environment and produce nothing but colemanballs... I wish life would be that easy, but it obviously is not. There is the firm representative coming in and out of discussion room and asking to see if you have made progress! Or rather to see if

there is any progress at all; the worst to see is misfocused group not knowing what to do or feeling in love with any colemanball version of any idea.

There are dedicated members of discussion rooms, staying in the room no matter how hopeless they are of any forseeable solution. But at least they try to the end, putting to work what they have accumulated in their math life time. There is no word for them. But there is another group wandering around the rooms trying to understand each problem while a little progress is already underway, so partially if not willingly, ruining the solution or bettering the peaceful study group process. Should the workers give him/her a credit and change their way of thought or not? Would it not be better if each group gathers around a naturally emerged group leader and follow his/her advices.

The hardest part, as always, is the modelling part. There you always have a problem, and obviously there are some models around that already met with dissatisfaction by the participating firms. You are asked to modify an existing model or come up with a completely new one. What is wrong with the one being used? Maybe it is the identification of what is important or not, or that the problem is associated with a new technology, or that it originated from having to do the best with the least effort, time, energy or so on. Here comes in the experience of senior researchers and thus the training part for the young participants. Every minute of it should be paid a great attention to. You will see how gravity loses its power at the fingers and words of such expertise. That is the part I myself enjoy the most about the study groups.

Next to hardest is actually not so hard. Once you have a model, everyone in the group will have an idea of how to handle it, be it a nondimensionalization or a suitable similarity transform or an asymptotic techique with or without matching with even a free boundary, numerics and so on. But then you will produce a graph or numbers that are supposed to make sense. It is actuallly the modelling part that will make it easy or hard to interprate what you have. I think you all will agree with me that it is easier to detect the wrong results of a correct model than the correct results of a wrong one.

Now comes the Friday morning, perhaps just when you wanted to work a little more to see if you could get anything further. Or, maybe it is good enough for the time being. Relax and see what the other groups also have come up with on seemingly horrible looking problems. Once solved or partially solved every problem looks so easy, is it not right?

Erhan Coşkun, Organizer

Department of Mathematics,

Karadeniz Technical University, TR-61080, Trabzon, Turkey

Acknowledgements

The financial support for the participants under age 35 came from TUBITAK. Karadeniz Technical University offered help with the local transportation of the participants, and the accommodation expenses of the invited participants. OCCAM(Oxford Centre for Collaborative Applied Mathematics) has covered the travelling expenses of the participants mainly from OCCAM. Participating companies have offered help in various ways.

On behalf of the executive committee, the organizer would like to also thank

Dr Orhan Fevzi Gümrükçüoğlu, Trabzon mayor,

Şefik Türkmen, Akçaabat mayor,

Suat Hacisalihoglu, chair, chamber of commerce and industry,Trabzon,

Hayrettin Hacisalihoglu, former deputy chair, Trabzonspor,

Prof. Dr Kenan İnan(former Dean), Prof. Dr. Mehmet Akbaş(Dean), Faculty of Science, Prof. Dr. Alemdar Bayraktar, Dean of Faculty of Engineering, and KTU administration.

The organizations and people above have made it easy for us to carry out this first study group in our country and they proved that mathematicians, engineers and industrial organizations can indeed come together and communicate very well.

Adaptive Light Control System

Problem Presenter

Mustafa Zihni SERDAR

Erişim Computer

Problem Statement

An adaptive traffic light system for crossroads is to be developed with the control being the data obtained through fixed cameras attached to the light system. The control itself is to be adaptive as there is no need for collecting data during the time when there is no traffic at all. Thus the problem is to collect data adaptively and control the light system accordingly. The idea, of course, is not to have people wait for unnecessary amount of time along the way, while there is no traffic across roads. Though looks rather reasonable, a very good adaptive strategy and an accompanying algorithm need to be developed. The study group is asked for such an algorithm. The problem requires collaborative work of mathematicians, computer scientists and electrical engineers.

Report authors

Ömer AKIN (TOBB Economy and Technology University)

Tahir KHANİYEV (TOBB Economy and Technology University)

İsmail KAYA(Karadeniz Technical University(KTU))

Orhan KESEMEN(KTU)

Contributors

Ömer AKIN(TOBB ETU),

Rovshan ALİYEV (KTU)

Fatma Gül AKGÜL(KTU)

Menşure CAN (KTU)

Fatma Zehra DOĞRU (KTU)

Ahmet GÖKDOĞAN(Gumushane University)

İsmail KAYA (KTU)

Gülay İlona TELSİZ KAYAOĞLU (MSGSU, Istanbul)

Orhan KESEMEN (KTU)

Tülay KESEMEN (KTU)

Tahir KHANİYEV(TOBB, ETU)

Mehmet MERDAN (Gumushane Univesity)

John OCKENDON (Oxford University, OCCAM)

George TURKIYYAH (America Uni. Lb)

Devran YAZIR (KTU)

The study groupe has identified two essential components of the problem:

maximize the traffic flow through the intersection and

minimize total waiting time at the intersection.

Both are formulated and combined into a single linear objective function with linear constraints by using appropriate relation between the density and speed.

1. Model

Given the lengths of the queues in four directions (obtained from camera images)

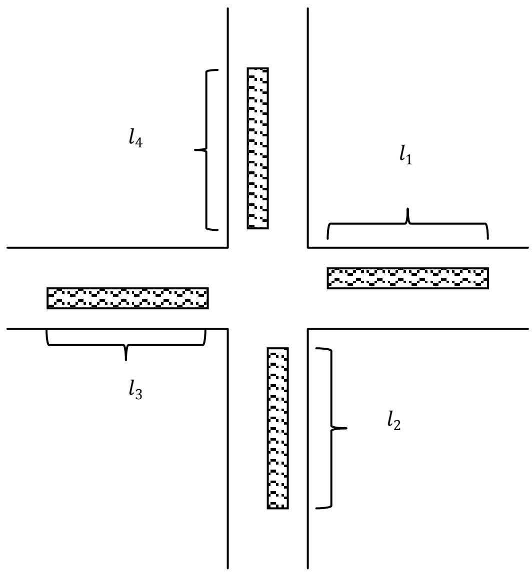

Figure 1. Final distribution of red and green lights for $E-W$, $N-S$ directions.

Aim-1

- Maximize flow through intersection

$$a)\ \sum_i \int_0^{t_i^{g\,(green)}} \rho_i v_i(t)dt \rightarrow maximize \tag{1}$$

or

$$\max\left(t_1^g v_1\rho_1 + t_2^g v_2\rho_2 + t_3^g v_3\rho_3 + t_4^g v_4\rho_4\right) \tag{2}$$

where ρ_i, v_i are the traffic density and velocity, respectively, in the $i-th$ direction as shown in Figure 1 and $t_i^{g\ (green)}$ is the duration of green light. The symbols E, W,N,S stand for the directions East, West, North and South.

We assume that

$$v_1 = v_2 = v_3 = v_4 = \bar{v} \tag{3}$$

so the maximization problem reduces to

$$t_1^g(\rho_1 + \rho_3) + t_2^g(\rho_2 + \rho_4) \rightarrow max \tag{4}$$

Aim-2

- Minimize the total waiting time

$$b)\ t_1^r \max(l_1, l_3) + t_2^r \max(l_2, l_4) \rightarrow minimize \tag{5}$$

If we define $l_{13} = \max(l_1, l_3)$and $l_{24} = \max(l_2, l_4)$ and the problem reduces to

$$(t_1^r l_{13} + t_2^r l_{24}) \rightarrow minimize \tag{6}$$

On the other hand, it is known that

$$t_1^r + t_1^g = T \tag{7a}$$
$$t_2^r + t_2^g = T \tag{7b}$$

So, the optimization problem becomes

$$t_1^g l_{13} + t_2^g l_{24} \rightarrow maximize \tag{8}$$

Thus, we have introduced two separate cost functions which are the minimum waiting time and maximum flow. These cost functions, Eq. (4) and (8), can be combined into

$$\alpha\big[\big(t_1^g l_{13} + t_2^g l_{24}\big)\big] + (1-\alpha)\big[t_1^g \rho_{13} + t_2^g \rho_{24}\big] \rightarrow maximize \tag{9}$$

Where $\alpha \in [0,1]$ ve $\rho_{13} \equiv \rho_1 + \rho_3$; $\rho_{24} \equiv \rho_2 + \rho_4$. It should be noted here that $t_1^g\ and\ t_2^g$are the unknowns to be determined throughout this optimization problem.

Constraints of the optimization problem:

1. $t_i^g \leq T$, i = 1,2,3,4 (10a)

2. $t_1^g = t_3^g$ and $t_2^g = t_4^g$ (10b)

3. $t_i^g \geq t_{min}$, if $l_i > 0$ (10c)

4. $\int_0^{t_i^g} \rho_i(t,x) v_i(t,x) dt \leq l_i$ (10d)

The constraints, (10a-10d), are set to maximize the objective function (9) in a realistic scenario shown in Fig.1. A linear programming method is suggested to solve (9),(10a-d) however constraint (10d) is not linear, as it stands. So, in order to reduece (9),(10a-d) to a linear programming problem, a relation between density and speed (ρ and v) is needed. For this reason the following continuous traffic flow model is considered.

2. Continuous traffic model

Let $\rho = \rho(x,t)$ and $v = v(x,t)$ represent density and velocity of traffic at the the position x and time t. Then the conservation law reads

$$\frac{\partial \rho}{\partial t} + \frac{\partial(\rho v)}{\partial x} = 0, \tag{11}$$

where $v = F(\rho, \rho_x, \rho_t, \dots)$.

(11) is a nonlinear hyperbolic PDE problem. We only need a linear relation between speed and density.

The following is a linear approximation for the required relation

$$v(t,x) = V_m \frac{\rho_m - \rho(t,x)}{\rho_m}, \tag{12}$$

where V_m and ρ_m are the maximal values of the speed and density.

Assume that, the light tuns into green at $t = 0$ and

$$\left.\begin{matrix} \rho = \rho_m \,; x \leq 0 \\ \rho = 0 \,; x > 0 \end{matrix}\right\} at\ t = 0$$

For $t > 0$ solution is called an expansion fan. In this case the density can be defined as $\rho(t,x) = F\left(\frac{x}{t}\right)$. In order to determine $F(z)$, $\rho(t,x) = F\left(\frac{x}{t}\right)$ and $v(t,x) = V_m \frac{\rho_m - \rho(t,x)}{\rho_m}$ are substituted into (11). Then the following relations are obtained:

$$\frac{\partial \rho}{\partial t}+\frac{\partial(\rho v)}{\partial x}=0 \Rightarrow \frac{\partial \rho}{\partial t}+v\frac{\partial \rho}{\partial x}+\rho\frac{\partial v}{\partial x}=0 \Rightarrow \tag{13}$$

$$-\frac{x}{t^2}F^{\prime}+V_m\left(\frac{\rho_m-F}{\rho_m}\right)\frac{1}{t}F^{\prime}+FV_m\left(-\frac{1}{\rho_m}\right)\frac{1}{t}F^{\prime}=0 \tag{14}$$

For $F^{\prime}\neq 0$, multiplying both sides of (14) with $\frac{\rho_m}{V_m}$ gives

$$-\frac{\rho_m}{V}\frac{x}{t}+\rho_m-F-F=0. \tag{15}$$

Then,

$$F\left(\frac{x}{t}\right)=\frac{\rho_m}{2}\left(1-\frac{x}{V_m t}\right) \tag{16}$$

or

$$\rho(t,x)=F\left(\frac{x}{t}\right)=\frac{\rho_m}{2}\left(1-\frac{x}{V_m t}\right) \tag{17}$$

is obtained as a *Fan Solution*.

Using (17), we obtain the following result:

$$\begin{aligned} v(t,x) &= V_m\left(\frac{1}{\rho_m}\frac{\rho_m}{2}\left(1-\frac{x}{V_m t}\right)\right) \\ &= \frac{V_m}{2}+\frac{x}{2t}=\frac{V_m}{2}\left(1+\frac{x}{V_m t}\right). \end{aligned} \tag{18}$$

Then the flow is obtained as

$$\rho(t,x)v(t,x)=\frac{\rho_m V_m}{4}\left(1-\frac{x^2}{V_m^2 t^2}\right). \tag{19}$$

The maximum flow is attained at the light position, $x=0$, and becomes

$$\rho(t,0)v(t,0)=\frac{\rho_m V_m}{4}. \tag{20}$$

If we substitute (20) into (10d), we have

$$\int_0^{t^g}\rho(t,0)v(t,0)dt=\frac{\rho_m V_m}{4}t^g \tag{21}$$

Using (21), the constraint (10d) becomes

$$\frac{\rho_{mi} V_{mi}}{4} t_i^g \le l_i, \quad i = 1,2,3,4 \tag{22}$$

Thus the new constraint equation (22) should be used instead of the constraint (10d). Then all the constraints would be linear in this optimization process. Therefore a linear programming method can be used to solve the optimization problem defined in (9) to determine the optimal values of t_1^g and t_2^g .

Since the method described above has been considered for very idealised form of the traffic light problem, it would be appropriate to express the view of the group for the general form of the traffic ligh optimization problem.

For example, the density function $\rho(t,x)$ can be discussed in the following figures for a real application.

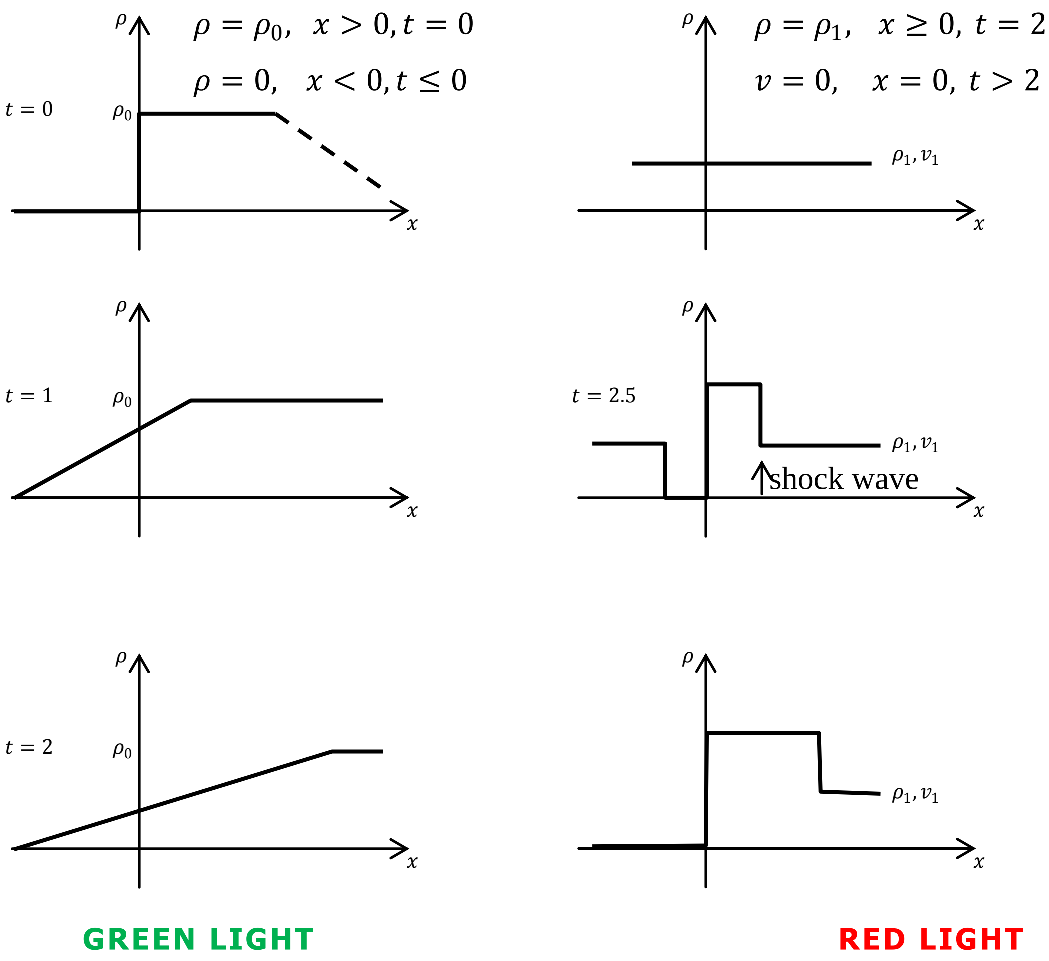

Figure 2 Various density distributions

On the other hand, general first-order conservation PDE is expressed as

$$\frac{\partial \rho}{\partial t} + \frac{\partial Q}{\partial x} = 0 \tag{23}$$

At a shock wave:

$$\left(\frac{dx}{dt}\right)_{shock} = \frac{[Q]}{[\rho]}, \qquad [F] = F^{+} - F^{-}, \ \ [\rho] = \rho^{+} - \rho^{-} \tag{24}$$

As an example, the cases subjected above can be discussed as following:

$$\rho^{+} = \rho_m \tag{25}$$

$$\rho^{-} = fan\, solution \tag{26}$$

$$Q = \rho v = V_m \rho \frac{\rho_m - \rho}{\rho_m}. \tag{27}$$

3. Conclusions

In this workshop, several aspects of traffic light optimization problem are discussed. The partial differential equation (11) is proposed to explain the relation between speed and density. (11) is based on the Haberman's method and helps to solve the traffic movements as it is in fluid dynamics. Finally, this report provides an accurate way to calculate how much time is required to finish a queeu when its length is known.

4. Recommendations

The problem of left turn is the next step to be solved.,

The relation between speed v and density ρ is assumed linear in this solution, however some nonlinear types of the relation could be included in this optimization, which is left for further studies.

The yellow light duration is fixed, so it may be excluded from the optimization process. Thanks for the yellow light duration which validates our solution and helps to make traffic light work.

5. Acknowledgements

The study group would like to thank Erhan COŞKUN (KTU, Turkey) for this workshop activity and the suponsors of workshop.

6. References

[1] Haberman, R., Mathematical Modeling, Prentice-Hall, New Jersey, 1998.

[2] Orosz, G., Wilson, R. E., and Stepan, G., (2010), "Traffic jams: dynamic and control", **Philosophical Transactions of The Royal Society, Series A,** Vol. 368 pp. 4455-4479.

[3] Dong L., Chen, W., (2010), "Real-Time Traffic Signal Timing for Urban Road Multi-Intersection", **Intelligent Information Management**, Vol. 2, pp. 483-486.

Spinning Soccer Ball Trajectory

Problem Presenter
Erhan Coskun[1]

Department of Mathematics, Karadeniz Technical University,

Trabzon, Turkey

Problem Statement

As can be remembered from the recent World Cup, uncertainities in the trajectory of a soccer ball at high speeds have led to some criticism on the ball manufacturers. The existing ball trajectory models assume that as the ball spins, a layer of air, say a boundary layer, follows the motion of the ball, thus spins with it. This, in turn, induces a velocity difference on the sides normal to ball's trajectory. The velocity difference then leads to pressure difference due to Bernoulli's principle. If $\vec{\omega}$ represents the axis of spin and $\vec{v}$ is the linear velocity, the resulting Magnus force would be in the direction of $\vec{\omega} \times \vec{v}$.

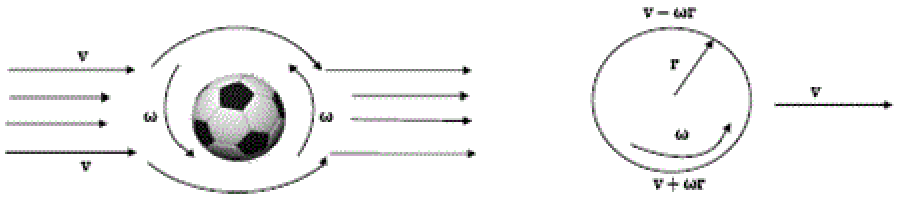

Figure. A soccer ball trajectory and the induced velocity difference

Yet, the resulting trajectory models do not seem to account for rapid changes in the trajectories. The study group is then asked to analyse the asumptions of the existing models and modify them if necessary to come up with a satisfactory model.

[1] The problem presenter gratefully acknowledges the motivational support of Hayrettin Hacisalioglu, a former deputy chair of Trabzonspor

[2] Hamit Cihan, a faculty member in Physical Education and Sport Department, KTU, who is also affiliated with Trabzonspor has provided valuable technical assistance to the studygroup upon the request of

Report Authors

Wan Chen(OCCAM,Oxford University, UK)
Bahadır Çor(Middle East Technical University, Ankara,Turkey)
Ali Konuralp(Celal Bayar University, Manisa, Turkey)
Tim Reis(OCCAM, Oxford University, UK)
Süleyman Şengül(Karadeniz Technical University, Trabzon, Turkey)

Contributors

Wan Chen(OCCAM,Oxford University, UK)
Bahadır Çor(Middle East Technical University, Ankara,Turkey)
Ali Konuralp(Celal Bayar University, Manisa, Turkey)
Tim Reis(OCCAM, Oxford University, UK)
Süleyman Şengül(Karadeniz Technical University, Trabzon, Turkey)
Hamit Cihan[2](Karadeniz Technical University, Trabzon, Turkey)
John Ockendon(OCCAM, Oxford University, UK)

EM2010, 1st Euroasian Studygroup with Industry,

04-08 October, 2010

was organized by Karadeniz Technical University, Trabzon, Turkey .

[2] Hamit Cihan, a faculty member in Physical Education and Sport Department, KTU, who is also affiliated with Trabzonspor has provided valuable technical assistance to the studygroup upon the request of Hayrettin Hacisalihoglu, a former deputy Chair of Trabzonspor.

Abstract

In this study the trajectory of a soccer ball is investigated using a dynamical system that takes the Magnus, drag and gravitational forces into consideration. In particular, close attention is paid to the trajectory of a soccer ball under an initial rotational kick. We first note that balls which are rather smooth, such as the Jabulani, typically hit the critical conditions of the so-called "drag-crisis" at crutial moments in a game of soccer, such as during a free-kick, so that "knuckling" is more pronounced. We then propose a simplified system consisting of three ordinary differential equations describing horizontal and vertical acceleration and rotation rate as functions of the forces on the ball, and of its "roughness". We find that the parameter controlling the roughness to play a critical role in the resulting trajectory. In particular, when this parameter is small, as we assume it to be for soccer balls such as the Jabulani, it is possible for the trajectory to develop two turning points, suggesting that the ball could appear to "bounce" in mid-flight.

1. Statement of the problem

As can be remembered from the 2010 FIFA World Cup, uncertainties in the trajectory of the Jabulani soccer ball has resulted in some criticism of the ball's design. Existing models for the trajectory of spinning soccer balls assume that a layer of air, known as a boundary layer, follows the motion of the ball, and thus spins with it. This, in turn, induces a velocity difference on the sides normal to the ball's trajectory. The velocity difference results in a pressure difference due to Bernoulli's principle. If ω represents the axis of spin and v denotes the (linear) velocity, then the resulting Magnus force would be in the direction of $\omega \times v$. However, the resulting models do not sufficiently account for rapid changes in the trajectories. The study group is thus asked to analyse the assumptions of the existing models and assess their validity.

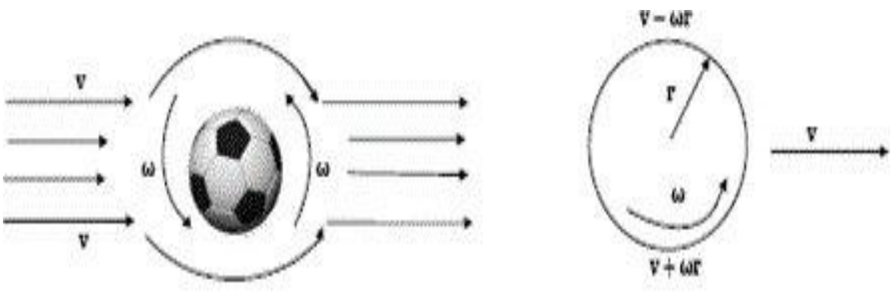

Figure 1: Velocity of a soccer ball.

2. Introduction and background

When a traditional soccer ball starts its descent, it is expected, due to the effect of gravity, to fall to the pitch without any reversal of its vertical velocity. However, the Jabulani has been observed to behave somewhat differently under certain conditions - after a forceful kick, soccer players have witnessed the ball moving upwards again shortly after the beginning of its fall; in other words, the ball's trajectory could have more that one maxima - "it's like putting the brakes on, but putting them on unevenly". This could clearly affect a player's ability to control the flight of the ball. From a goalkeeper's viewpoint, an approaching ball may suddenly appear to change its direction in a way grossly unpredictable. We believe this kind of phenomenon, arguably a much more common (and unwanted) attribute of the Jabulani, is related to the amount of, and indeed pattern of, the surface roughness of the ball. This in turn will affect the position of the separation points of the boundary layers, which are a feature rotating flows. Some specifications of a traditional soccer ball and the Jabulani ball are compared in Table 1. Although this table appears to show that the Jabulani has improved, more advanced, features, some of those who have used this ball at a competitive or professional level have criticised its controllability and dynamics.

	Standard FIFA approved ball	Jabulani
Circumference (cm)	68.5-69.5	69.0±0.2
Weight (g)	420-455	440± 0.2
Change in diameter (%)	≤1.5	≤1
Water absorbtion (weight increase, %)	≤10	1
Rebound test (cm)	≤10	≤6
Pressure loss (%)	≤20	≤10

Table1: Technical specification of standard FIFA approved soccer balls and the Jabulani ball.

The dynamics of a soccer ball in flight is closely related to a classical problem in theoretical fluids mechanics, namely the flow around a rotating sphere. For clarity, let us first consider a smooth cylinder of radius a in a stream with velocity U of ideal fluid with circulation Γ. The streamfunction in polar coordinates (r, θ) for this flow can be found to be [1]

$$\psi = Ur\sin\theta - \frac{Ua^2\sin\theta}{r} - \frac{\Gamma}{2\pi}\ln\frac{r}{a}, \tag{1}$$

If $\Gamma \leq 4\pi Ua$, there is a stagnation point on the cylinder and from Bernoulli's principle it can be found that the drag F_D and lift F_L forces are respectively given by

$$F_D = 0, \tag{2}$$

$$F_L = -\rho U\Gamma, \tag{3}$$

where ρ is the density of the fluid. The lift force can be understood as follows: The circulation gives higher speed on one side of the cylinder (c.f Figure 1). This higher speed is associated with lower pressure p since

$$p + \frac{1}{2}\rho v^2 = \text{constant}, \tag{4}$$

and hence there is a force, known sometimes as the Magnus force, from the high pressure (slow speed) side to the low pressure (fast speed) side. So a soccer ball kicked with sufficient spin will generate lift and rise. As the ball slows its trajectory will be altered by the forces acting on it and curls upon descent, as is observed in, for example, free-kick taking. However, there are considerable viscous effects near the boundary of the cylinder/sphere and hence Bernoulli's principle loses its validity. The body may be subjected to turbulence, which can affect it's flight. Note that although this alters the forces on the sphere, the physical intuition remains. In this more complicated, yet more interesting and realistic case, the forces acting on the body are given by

$$F_D = -\frac{1}{2}C_d\rho A|v|^2 e_x, \tag{5}$$

$$F_M = -2C_d\rho A|v||\omega|e_y, \tag{6}$$

$$F_g = Mg, \tag{7}$$

where C_d is the drag coefficient, ρ is the fluid (air) density, A is the cross-sectional area of the ball, M is its mass, and $g = 9.8\,\mathrm{m/s^2}$ is the gravity. The drag coefficient C_d will depend on the properties of the ball and the Reynolds number, Re, which is defined to be

$$\mathrm{Re} = \frac{|\mathrm{v}|\mathrm{L}}{\mathrm{v}}, \tag{8}$$

where v is the fluid's kinematic viscosity and L is a characteristic length, which is taken to be the diameter of the ball. Moreover, at high Reynolds numbers, boundary layers are present and flow separation is observed at two separation points on the cylinder. In the absence of rotation these separation points are symmetric with respect to the azimuthal coordinate (see Figure 2, for example) and asymmetric when the cylinder/sphere is spinning.

The displacement of the line of separation has a considerable effect on the flow. In Figure 2 the separation points are close together so that the turbulent wake beyond the body is contracted. This, in turn, reduces the drag experienced by the body. Thus the onset of turbulence in the boundary layer at larger Reynolds numbers is accompanied by a decrease in the drag coefficient. When the separation points are further apart the drag increases significantly (this is sometimes referred to as the drag crisis [2]). In other words, causing a turbulent boundary layer to form on the front surface significantly reduces the sphere's drag. In terms of soccer balls, for a given diameter and velocity the manufacturer has just one option to encourage this transition: to make the surface rough in order to create turbulence. We note that the same principal applies to golf balls.

Although the mathematics and physics of rotating bodies is complicated, we develop a simple dynamical system to describe the trajectory of such a body that is affected by acceleration, spin, and surface roughness. Despite its simplicity it can highlight the motion of a soccer ball and the critical features that can cause unexpected or unwanted behaviour. We point the interested reader to other works in this field [4, 5, 6, 7].

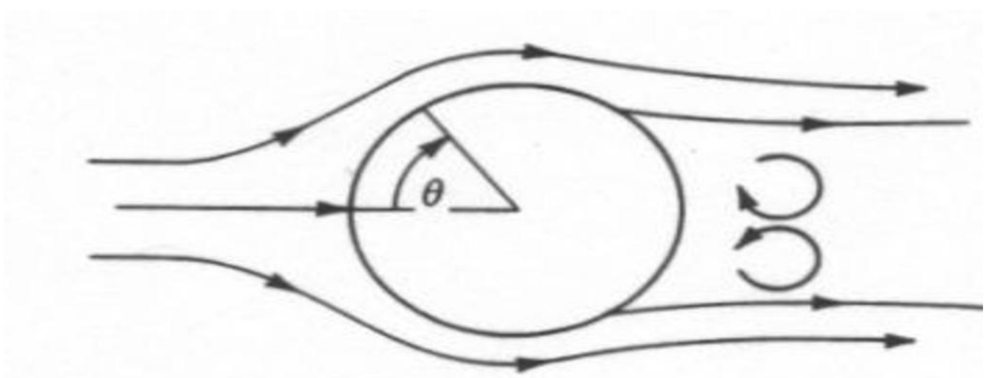

Figure 2: The general character of flow over a cylinder at high Reynolds numbers.

The remained of this report is structured as follows: In Section 3 we note some observations we have made related to the flight of the Jabulani; in Section 4 we present the dynamical system for the trajectory of a rotating cylinder; the results are presented in Section 5 and a summary is drawn in Section 6.

3. Observations

The relationship between the drag coefficient and Reynolds number for smooth and rough spherical bodies is shown in Figure 3.

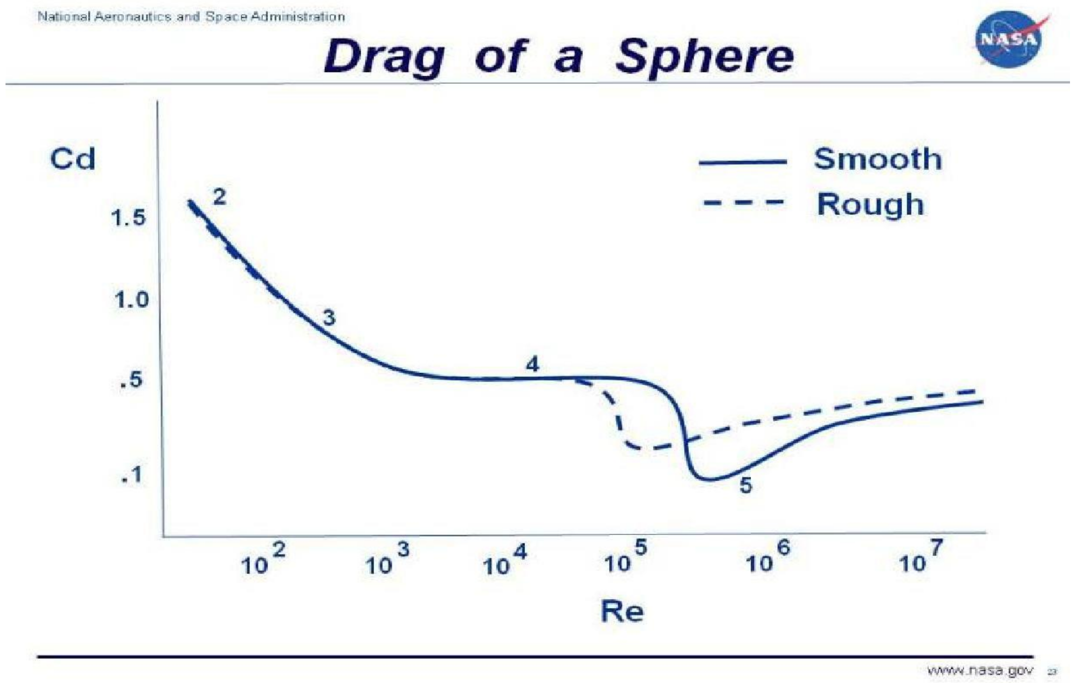

Figure 3: Drag coefficient for rough and smooth spheres.

Traditional soccer balls are not smooth. Although some surface roughness has been added to the Jabulani it is still a lot smoother than other soccer balls. It is therefore reasonable to assume that the dynamics of each will differ, especially when rotation is included. Also, traditional balls have a hexagonal design and at small spin the stitching can cause an a asymmetric flow field, causing the ball to "knuckle"; that is it may be pushed a small amount in a given direction even when the ball has little rotation. The Jabulani has no stitching and the speed at which knuckling may occur is $20 - 30\,\mathrm{km/h}$ faster with the Jabulani than with traditional balls [3]. This coincides with the average speed of a free kick, and hence the pronounced visibility of chaotic trajectories with the Jabulani.

During its flight, the highest measured speed of a soccer ball kicked by a player in an official game is $140\,\mathrm{km/h}$. A typical powerful shot kicked by a professional player (during a free-kick, for example) gives the ball a speed of about $100\,\mathrm{km/h}$ (about $30\,\mathrm{m/s}$). With the known values of v (roughly $20\times10^{-6}\,\mathrm{m^2/s}$) and L, we calculate the Reynolds number in to be between between $100\,000$ and $500\,000$. From Figure 3 we can see that the drag coefficient of the rough ball does not drop as dramatically as the smooth one in this regime. Although the Jabulani does have some surface roughness, it is still considerably smoother than any other soccer ball. Therefore the Jabulani may experience rapid changes in the forces acting on it during high Reynolds number flows, such as during a free kick.

We also note that the distribution of surface roughness is likely to effect the flow field around a rotating body. Old soccer balls may have stitching which could potentially alter the flow field, but the stitching is evenly spread over the surface area. It is not obvious if the small roughness that has been added to the Jabulani is equally distributed over the ball. Indeed, an eye-ball examination would suggest otherwise. Although this is unlikely to have an effect in most situations it may well be an important factor that needs consideration when the ball is rotating at high Reynolds numbers.

4. The proposed model

We developed a simple, idealised, dynamical system for the trajectory of a cylindrical body that takes surface roughness into consideration. The governing system is written as

$$\ddot{x} = -\frac{1}{2m}C_d\rho A\dot{x}\sqrt{\dot{x}^2+\dot{y}^2} - \frac{2\rho Ar}{m}C_d\dot{y}\omega\,, \tag{9}$$

$$\ddot{y} = -\frac{1}{2m}C_d\rho A\dot{y}\sqrt{\dot{x}^2+\dot{y}^2} + \frac{2\rho Ar}{m}C_d\dot{x}\omega - g, \tag{10}$$

$$\dot{\omega} = -\frac{R}{r}\sqrt{\dot{x}^2+\dot{y}^2}\,\omega, \tag{11}$$

subject to the following initial conditions:

$$x(0) = 0;\ x'(0) = 30, \tag{12}$$

$$y(0) = 2;\ y'(0) = 0, \tag{13}$$

The initial conditions for ω will be discussed in the following section. In the above, R is a parameter (assumed constant) describing the roughness of the ball, r is the radius and x, y and ω are functions of time (t). We assume the drag coefficient undergoes a rapid change in the critical Reynolds number regime and fit it using a cubic interpolation from Figure 3, that is

$$C_d = 0.0198\left(\frac{Re^3}{3} - \frac{7Re^2}{2} + 6Re\right) + 0.457, \tag{14}$$

The other parameters were chosen according to the physical characteristics:

$$m = 0.44 \text{ kg},$$

$$r = 0.1098 \text{ m},$$

$$\rho = 1.225 \text{ kgm}^{-3},$$

$$A = 0.037875167 \text{ m}^2,$$

$$v = 2 \times 10^{-5} \text{ m}^2\text{s}^{-1}$$

The first two equations in our system my be viewed as statements of Newton's second law of motion, i.e force = mass×acceleration, where the horizontal and vertical forces are taken from equations 5 and 6. Equation (9) describes the horizontal acceleration in terms of the drag force. We see that the equation for vertical motion, equation (10), has three terms; the first two of these (which correspond to the Magnus, or lift, force) must exceed the last (which is describing the action of gravity) if there is to be an upwards motion. It should also be noted that the second terms in equations (9) and (10) depend on the rotation, ω, which itself depends on the roughness parameter R.

5. Results: Trajectory of the ball

We consider the trajectory of smooth and rough balls with different initial conditions. That is, we solve the dynamical system given my equations (9)-(11) subject to $\omega(0)$. When R is relatively large, or when the ball is "rough", the gravity term dominates the solution for the vertical path and, once the ball has reached its maximum height (here there is only one local maximum of the trajectory), it starts to uniformly descend, as shown by the dash-dotted line in Figure 4. This is what one would expect if playing soccer with a sensible ball in sensible conditions. Similar results are obtained even when the ball is given a relatively hefty rotational kick ($\omega(0) \sim 50$) but will behave curiously for excessively (unrealistic) large initial vales of ω. If we reduce R, which corresponds to a smoother ball, a sufficiently (but not excessively) large amount of initial spin can cause the body to generate a secondary lift (Magnus force) as it begins its descent, which actually causes it to rise again briefly – a phenomena that has been observed with the Jabulani and predicted by Figure 4 (solid line) and Figure 5 using our model. The dotted line in Figure 4 is the predicted trajectory when $R = 0.00002$ and $\omega(0) = 50$ – that is, a very smooth ball with large initial rotation. In this case we see a steep rise to a global maximum of the trajectory, which is beyond (and higher than) the local maximum of a standard parabolic curve under comparable conditions. This is an extreme case and may not be realisable in practise.

For further insight we plot the velocity and acceleration for different values of R when $\omega(0) = 50$ in Figures 6 and 7, respectivley. The increase in the velocity and decrese in acceleration when R is small is noteworthy since it may be

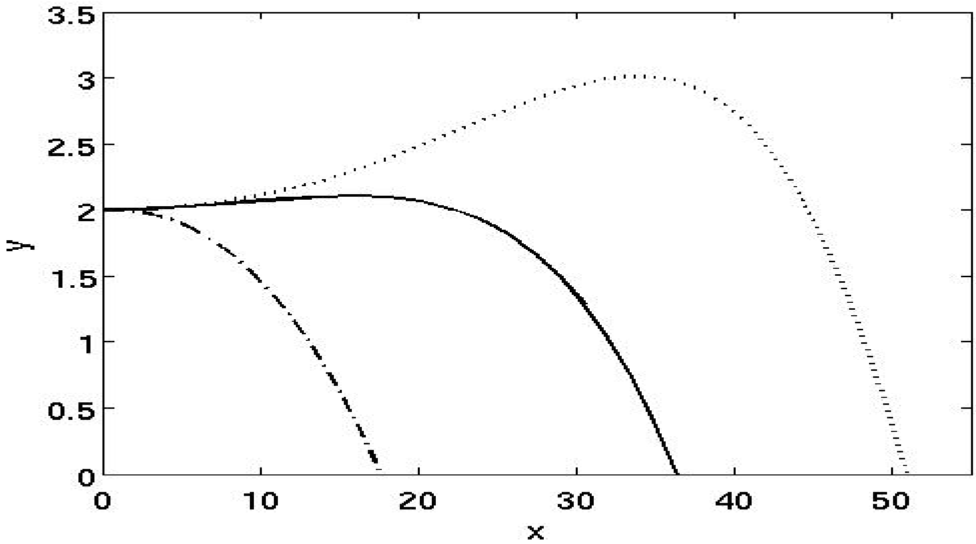

Figure 4: The $x - y$ trajectory of a spinning ball when $R = 0.00002$ (dotted), $R = 0.002$ (solid), $R = 0.2$ (dash-dotted) with initial angular velocity $\omega = 50$.

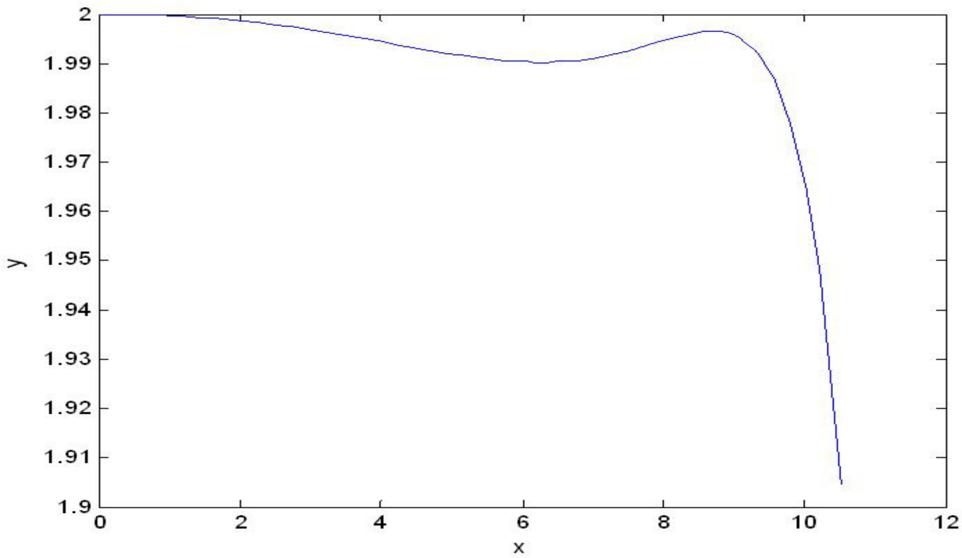

Figure 5: The $x - y$ trajectory of a spinning ball obtained from our dynamical system.

counter-intuitive and certainly not what one expects with traditional, rougher, soccer balls (c.f dot-dashed lines in Figures 6 and 7).

We mentioned above that the initial conditions (in partcular, the initial rotation) also affect the flight path, and this can be seen in Figures 8, 9 and 10. Figure 10 is particuarly enlightening since it shows the complicated, highly non-linear behaviour of the acceleration for a smooth ball, even when the initial rotation is relatively small.

6. Discussion

We have proposed a dynamical system to predict the trajectory of a cylindrical body subject to acceleration, spin, and surface roughness. We have shown that the roughness (included through the parameter R) and the initial spin to be the critical factors responsible for the so-called "knuckling" effect, and for unpredictable changes in a balls vertical acceleration. This could offer some understanding to why the Jabulani, a smoother-than-normal ball, exhibits somewhat unpredictable behaviour under crucial conditions such as free-kick taking, long-range passing, and distance shooting. Physically, the roughness parameter R is related to not only the surface structure of the ball but also the separation points of the boundary layer during rotational flow. Small R will be accompanied by widely spaced separation points and a large turbulent wake, whereas a larger R means the separation points will be closer and the wake behind the sphere narrower. A potentially interesting further study could be to try and quantify this relationship, perhaps by introducing a fourth equation for the symmetry of separation or to include the "spread" of roughness (for example, as noted above it is not clear if the roughness purposefully added to the Jabulani is sufficiently, or evenly, distributed over the ball's surface). Perhaps a model with a variable R may also be enlightening. We have also remarked that the forces on the Jabulani may undergo rapid changes (more rapid than for rougher traditional balls) during a free kick, which will effect its flight kinematics. It is also worth mentioning that an experimental study [3] revealed that the new ball falls victim to "knuckling" at higher velocities than old soccer balls, which coincides with the average maximum speed of flight during a free kick. It is unclear if the knuckling effects are stronger with the Jabulani, or just more readily observed. Considering free kicks and high

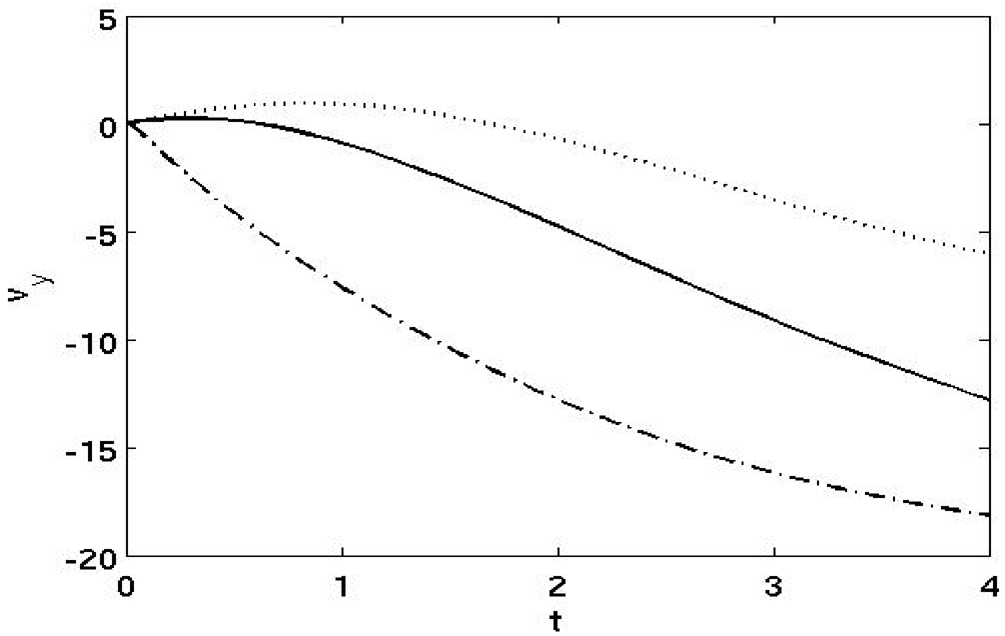

Figure 6: The vertical velocity of a spinning ball when $R = 0.00002$ (dotted), $R = 0.002$ (solid), $R = 0.2$ (dash-dotted) with initial angular velocity $\omega = 50$.

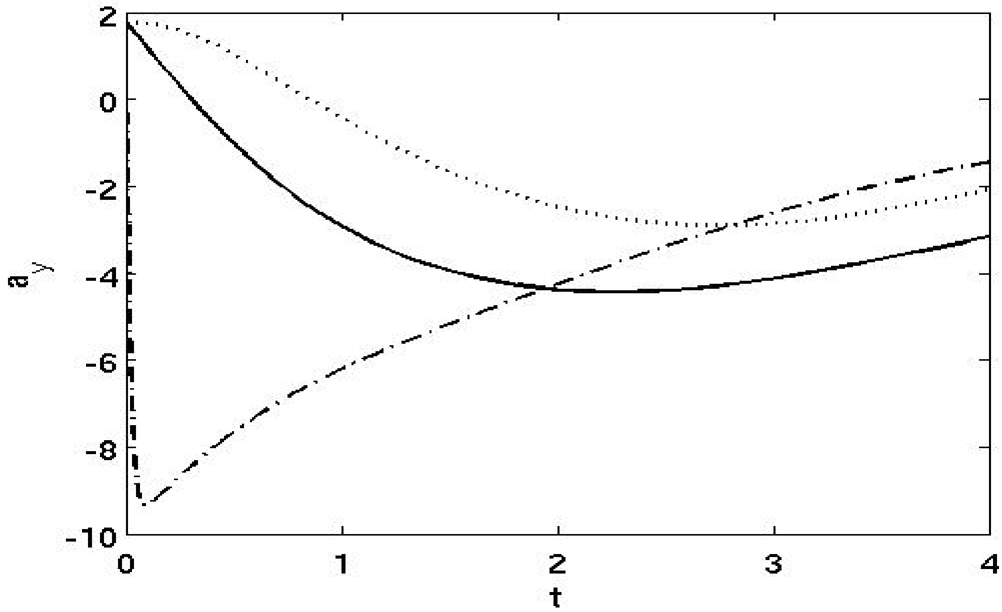

Figure 7: The vertical acceleration of a spinning ball when $R = 0.00002$ (dotted), $R = 0.002$ (solid), $R = 0.2$ (dash-dotted) with initial angular velocity $\omega = 50$.

velocity passing and shooting are crucial elements of soccer, one would desire to have maximum control during these critical moments.

Acknowledgments

We would like to thank Dr. Erhan Coşkun of Karadeniz Technical University for organising the first Euroasian study group. TR and WC would also like to thank the Oxford Center for Collaborative Applied Mathematics (OCCAM) for their support.

References

[1] G.K. Batchelor, An Introduction to fluid mecahnics Cambridge Univeristy Press, 1973.

[2] L.D. Landau and E.M Lifshitz, Fluid Mecahnics, Pergamon Press, 1987.

[3]NASA report,

http ://www.nasa.gov/topics/nasalife/features/soccerball.html.

[4] J.E. Goff and M.J. Carre, Trajectory analysis of a soccer ball, Am. J. Phys, 77(11), 2009.

[5] J.E. Goff and M.J. Carre, Soccer ball lift coefficients via a trajectory analysis, Eur. J. Phys, 31. 2010.

[6] S. Şengül, Trajectory Model of a Soccer Ball and Analysis, MSc Thesis, Karadeniz

Technical University, Trabzon, 2011.

[7] R. D. Mehta and J. M. Pallis. Sports Ball Aerodynamics: Effects of Velocity, Spin and Surface Roughness, Materials and science in sports, IMS 2001.

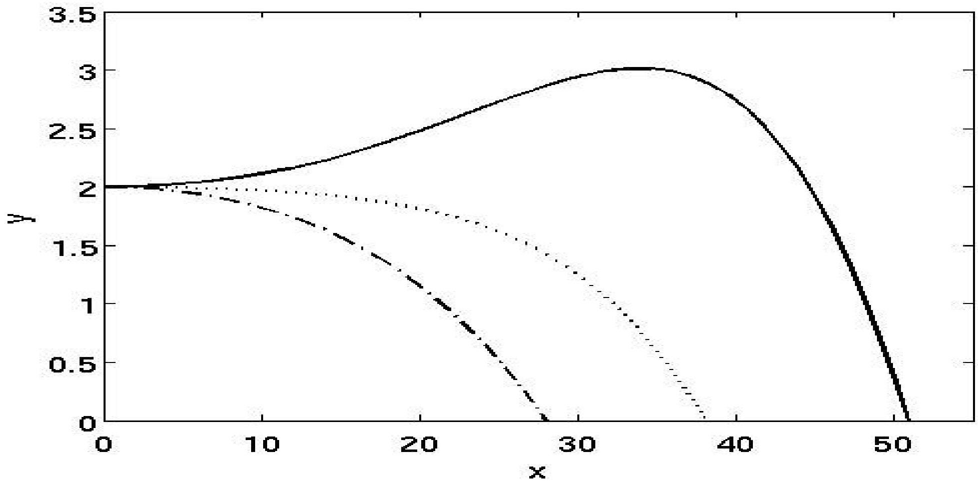

Figure 8: The $x - y$ trajectory of a spinning ball when $\omega = 50$ (solid), $\omega = 40$ (dotted), $\omega = 30$ (dash-dotted) with roughness parameter $R = 0.00002$.

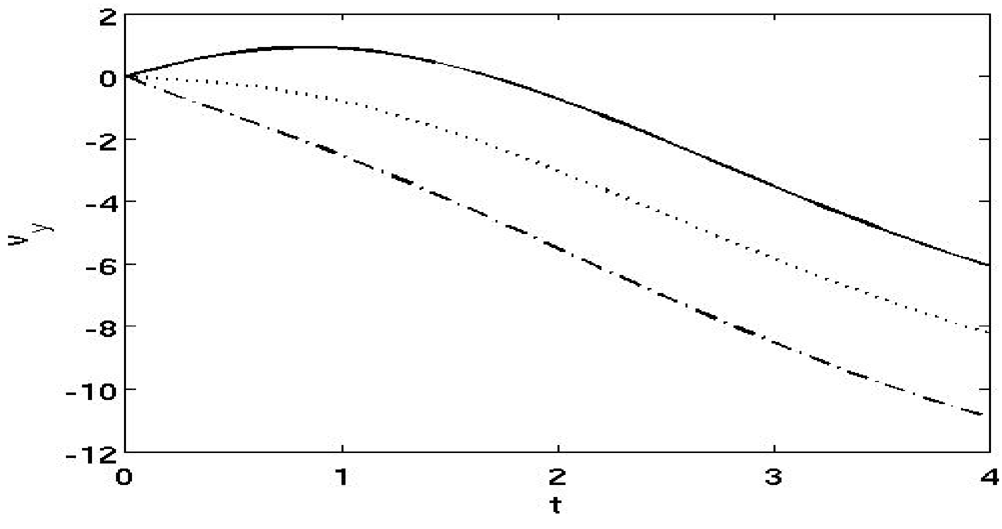

Figure 9: The vertical velocity of a spinning ball when $\omega = 50$ (solid), $\omega = 40$ (dotted), $\omega = 30$ (dash-dotted) with roughness parameter $R = 0.00002$.

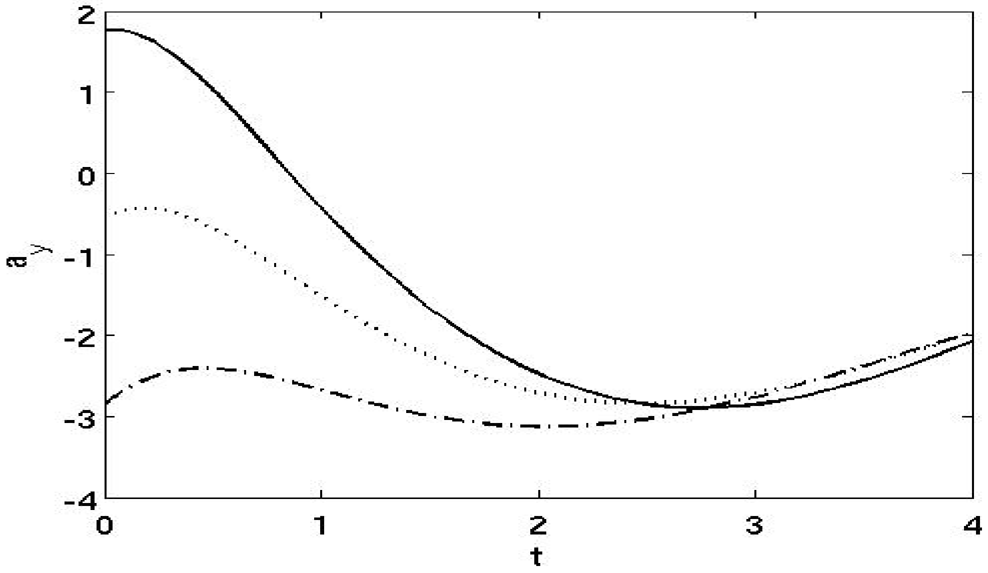

Figure 10: The vertical acceleration of a spinning ball when $\omega = 50$ (solid), $\omega = 40$ (dotted), $\omega = 30$ (dash-dotted) with roughness parameter $R = 0.00002$.

Handgun Accuracy Problem

Problem Presenter

Murat Alemdaroglu

Problem Statement

A laboratory test, aimed to check the compliance of the model with demand, indicates that consecutive fires of about 10 centers around a circular region with a radius of 10cm. The fact that the fires, though performed at the same conditions, do not target at the same point is called focusing uncertanity of the handgun. Furthermore, it is observed, by myself also, that bullet velocity measured 10 metters from gun varies up to about 7m/s(around 340m/s) among the firing set of 10. There are about ten different models and each model seems to display a different magnitude of uncertanity and velocity deviation from the expected average. The company, being willing to produce more data at request, asks to see if the focusing uncertanity and variation in bullet velocities can some how be corelated. And with some help from other disciplines, the fact behind such uncertainities..? Experiment apparatus or manufacturing process. If latter, which manufacturing unit contributes more?

Report authors and contributors

Ellis Cumberbatch (University of Claremont Graduate)

Ali Konuralp (University of Celal Bayar)

Onur Köksoy (University of Nigde)

The problem statement submitted read as follows

1.A handgun problem

A handgun manufacturer located in Trabzon aims to meet demands of people of Blacksea and abroad with a variety of models such as Kanuni, named after Kanuni Sultan Süleyman or better known Suleyman the Magnificant who was born in Trabzon, and Zigana, named after high mountains nearby Trabzon. The company would like to optimize its production reinvestigating the models at hand:a statistical and a modelling approach seems to be needed for their request initially.

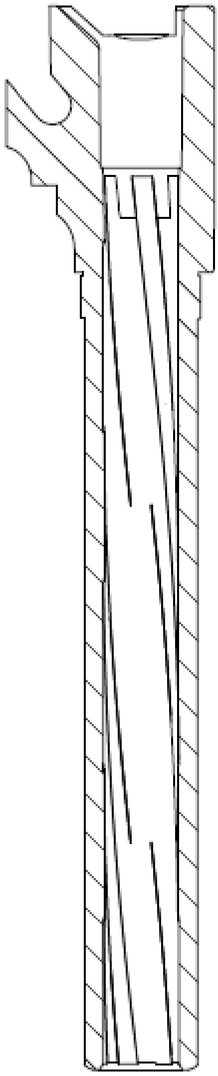

A laboratory test, aimed to check the compliance of the model with demand, indicates that consecutive fires of about 10 centers around a circular region with a radius of 10cm. The fact that the fires, though performed at the same conditions, do not target at the same point is called focusing uncertanity of the handgun. Furthermore, it is observed, by myself also, that bullet velocity measured 10 metters from gun varies up to about 7m/s(around 340m/s) among the firing set of 10. There are about ten different models and each model seems to display a different magnitude of uncertanity and velocity deviation from the expected average. The company, being willing to produce more data at request, asks to see if the focusing uncertanity and variation in bullet velocities can some how be corelated. And with some help from other disciplines, the fact behind such uncertainities…? Experiment apparatus or manufacturing process. If latter, which manufacturing unit contributes more?

2. Introduction

The problem described by the manufacturer's presenter concerned the accuracy of the standard handgun. This accuracy was measured in the company's firing range, which was visited twice by workshop participants. The gun is held in a vice, ten bullets are fired in a test, each bullet being manually placed in the chamber and the hole it makes in a paper target 25 meters away marked by an operative. The bullet's speed 3 meters from the muzzle is also measured. Bullet holes on the paper target can be up to 15cm apart (with no preferred axis) and the speed can vary by 18 m/sec. (Example: 355 +_ 9 m/sec.) Comparison of a number of 10-shot tests did not suggest any particular trends, or correlations, between speed variations and angle dispersion. (See Figure 2.) The only noticeable feature was that the first shot fired tended to be on the outside region of the ten on the target paper. The workshop problem was to identify possible mechanisms that give rise to the dispersion of speed and angle and to model those mechanisms so that corrective design changes could be implemented.

In the following sections we provide the specifications of the gun that was used in the test firings and that was analyzed. Then we list the various mechanisms involved in firing the bullet, their likelihood of causing dispersion both in speed and angle of bullet trajectory, and suggestions for tests that could narrow the choice of causes.

3. Gun Specification

The standard handgun has the following technical specifications: 9×19 mm. caliber, simple recoil system, semi-automatic, magazine Capacity:15/18/20, triggering system: double action, total pistol weight (Empty Magazine):942 gr. (±10 gr.), operating temperature:-35 °C / +60 °C, barrel rifling: right hand twist, 6 lands and grooves, length of twist:250 mm. The gun is shown in Figure 1.

Figure 1. The standard handgun. 9×19 mm calibre

Rifling refers to the helical grooves on the interior surface of the barrel. As the bullet is forced into the barrel by the high pressure created by the gunpowder explosion, the soft metal on the outer surface of the bullet is forced to conform to the cross-sectional shape of the barrel. The helical rotation of this shape on the inside of the barrel then causes the bullet to spin, and in its trajectory in free flight the spin improves its aerodynamic stability. The internet provides numerous references to rifling, e.g. http://en.wikipedia.org/wiki/Rifling. Some rifling patterns are shown in Figures 9 and 10. There was no time during the workshop for the helical motion of the bullet inside the barrel to be considered.

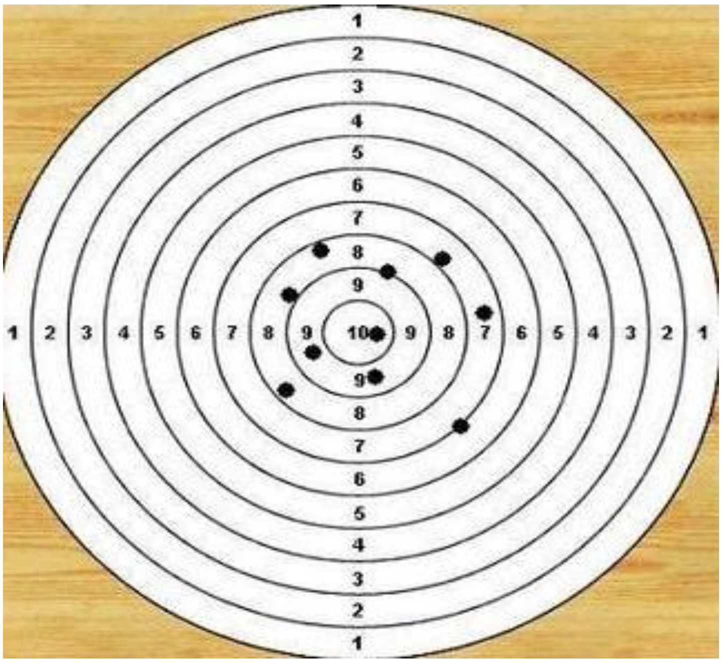

Figure 2. An example paper shot ten times successively.

4. Problem Approach

On the afternoon of the first day interested participants became acquainted with the gun's components and mechanisms (few of us had any experience in these.) The components of the handgun are shown in Figure 3 and the bullet/cartridge in Figure 4.

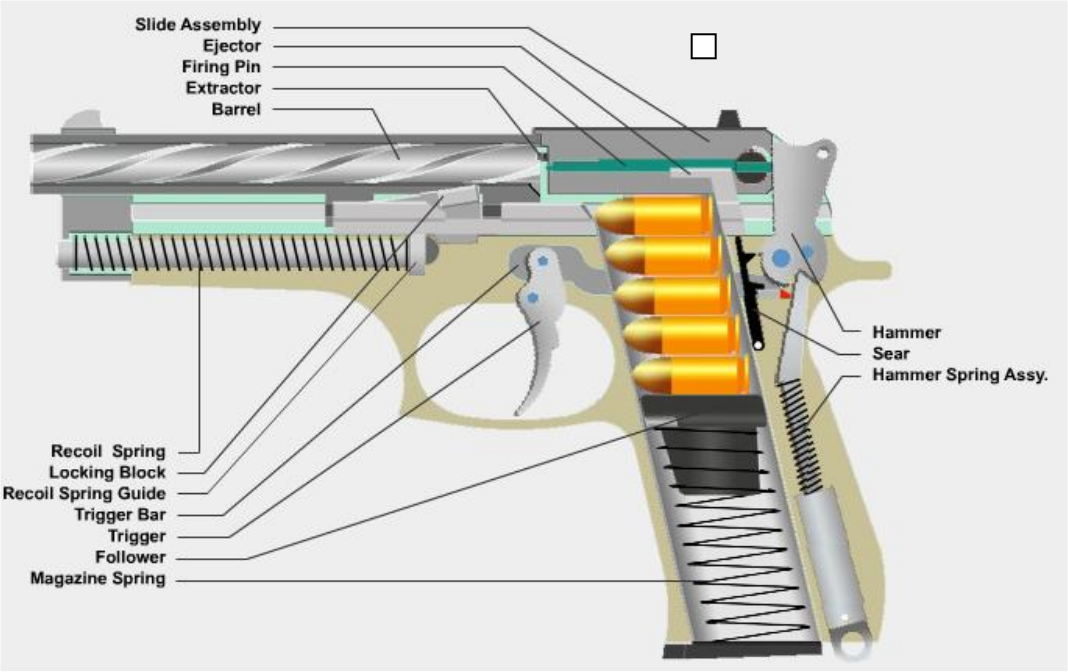

Figure 3. Primary components of the standard handgun

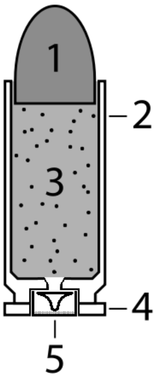

A modern cartridge consists of the following:

1. the bullet itself, which serves as the projectile;

2. the case, which holds all parts together;

3. the propellant, for example gunpowder or cordite;

4. the rim, part of the casing used for loading;

5. the primer, which ignites the propellant.

Figure 4. A modern cartridge

Activating the trigger allows the hammer to hit the primer which then ignites the gunpowder, causing an explosion and a large rise in pressure which forces the bullet down the barrel. The cartridge, being of large diameter than the barrel interior, remains in the firing chamber to be ejected subsequently. The bullet accelerates down the barrel and leaves the muzzle followed by the hot explosion gases. A new bullet may be inserted manually into the chamber; if there is a magazine clip, housed in the gun handle, each bullet in the clip is pushed into the chamber by force of a spring. The momentum of the bullet imposes a force in the opposite direction on the gun. This is partially absorbed by the recoil spring, to be released later as the assembly returns to its former state.

For the test firings, no bullet clip is inserted into the handle. The gun is held in a large, heavy, cast-iron vice, whose shaft fits through the handle. The faces of the vice clamp the gun on its handle just below the barrel/recoil spring assembly. On firing the vice slides slowly backwards on rails, approximately 2 cm., reacting to the recoil. The vice/ rail assembly is very stable and secure, with no visible vibration at a firing.

During the initial introduction to the mechanics involved in the firing of a bullet, and subsequently, a number of possible causes for angle and speed scatter were suggested. The primary ones that were discussed are listed below:

1. Differential heating (in space and time) of the gun barrel caused by the heat of explosion from each of the ten firings.
2. Recoil spring motion.
3. Interaction between the firing explosion and the motion of the vice.
4. Motion of the barrel assembly during firing.
5. Variability of bullets. The gun manufacturer is supplied with bullets by an outside manufacturer and there did not seem to be any data on their variability. (The latter is restricted in some manner by Turkish government regulations.) Variability in gun powder quality and in the amount inserted in each cartridge is clearly a possible cause of speed scatter, as is variability in manufacture of the bullet casing causing weight changes or distribution. The workshop had no resources to assess these and these aspects are left to the gun manufacturer to research. The other four possible causes above are now analyzed.

5. Analysis

5.1 Heating

This effect was discounted during the first visit to the firing range. Neither the ejected cartridge nor the gun barrel registered any substantial change in temperature after a firing, nor after ten firings. A fired cartridge was slightly warm to the touch. We had anticipated quantifying the amount of heat generated during a firing. This is possible from general information regarding the physics of firearms (see http://en.wikipedia.org/wiki/Physics_of_firearms#Firearm_energy_efficiency) that provides an energy distribution into approximately equal parts between bullet motion, temperature rise in the barrel and bullet, and heat content in the exhaust gases. Since we can deduce the bullet energy, the other two can be estimated. Temperature effects were not pursued subsequently.

5.2 Recoil spring motion

No exhaustive analysis was attempted for this effect. However, in order to give some partial information on the effects of the recoil spring (a mechanism to bring the barrel back to its rest position) on speed and angle control, we tried two different recoil springs in a standard handgun, that are called soft and hard springs. For tests consisting of two successive firing sets of 10, the diameters of bullet holes on the target sheets were 9.5cm and 9cm, respectively, not indicative of any major change different from the scatter on other tests. The recoil spring developed for a superior design and functionality called a "frame saver dual action recoil buffer spring system" is shown in Figure 5. It has several advantages such as preserving the structures of the handgun from the slide impacting the frame at high speed, gaining more control after the shot, better stability of the barrel and so on.

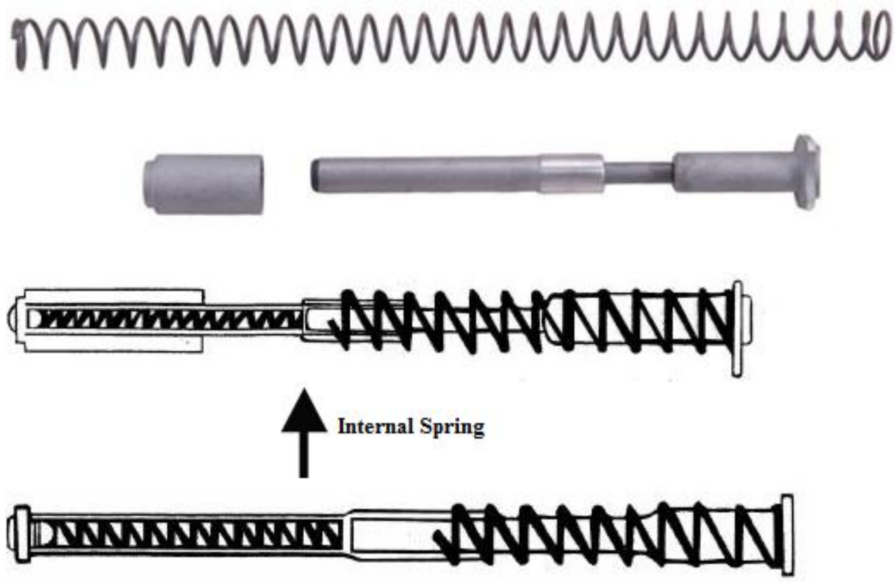

Figure 5. A frame saver dual action recoil buffer spring system and its structure.

5.3 Vice motion.

It was conjectured that the explosion could give rise to a vibration of the vice that in turn would cause movement in the gun position thereby affecting the bullet trajectory. This was discounted as a result of the **sugar cube experiments**, now described.

.

Figure 7. Sugar cube test, before, during and after firing:

Sugar Cube Experiments. In order to take into consideration the movement of the handgun and vice generated by the explosion during the firing, we placed sugar cubes at various positions on the barrel and vice, watched their motions and took video recordings. The sugar cubes, available in restaurants, were light and were wrapped in a waxy paper so that there was little friction between the cube and the surface on which it is placed. In Figure 7 some frames from the videos illustrate placement of the cubes and their subsequent motion during firing. There was upwards movement of the sugar cubes placed on the barrel, about 10 cm. into the air for a cube placed near the muzzle, half that for a cube placed mid-way from muzzle to chamber. The video frames in Figure 7 show that the movement of the cube takes place after bullet has left the barrel and that cubes placed on the vice do not move.

The sugar cube experiments for cubes placed at various locations on the barrel and vice showed no motion at all of those placed on the vice even though the cubes on the gun barrel exhibited a substantial jump. The vice has a slow rear-wards recoil motion which had no effect on the cubes. As a consequence of this it was decided that the vice played no role in the bullet trajectory scatter.

5.4 Barrel assembly motion during firing

The sugar cube experiment indicates that the explosion causes a reaction in the barrel assembly and this results in an impulsive moment to the assembly. Possible causes are now discussed.

(a) The gun powder explosion causes elastic wave motions in the gun material: here the discussion will be restricted to the barrel assembly. Longitudinal, transverse (shear), surface and toroidal waves are all possible. In steel, the wave speeds of the first three of these are 5,900, 2,300, 2,100 m/sec, respectively. (Toroidal wave speeds depend on the cross-sectional shape of the barrel, and since the cross-section is not a simple structure, this will not be considered.) The bullet speed at the muzzle is approximately 350 m/sec, and since the acceleration to this speed has been from rest, the average speed along the barrel is less than this. (If the bullet mechanics down the barrel are approximated by a constant acceleration, the average speed is 2/3 the final speed.) It is evident from the large ratio of the elastic wave speeds to the average bullet speed that the elastic waves have had time to reflect eight or ten times back and forward along the gun barrel before the bullet exits and the sugar cube jumps. So attributing the phenomenon exhibited by the sugar cube experiment to elastic waves of the gun barrel is very unlikely. However we now conjecture a related mechanism of the elastic wave motions:

(b) A close examination of the barrel assembly revealed that the gun barrel fits in a cylyndrical, concentric sleeve, the barrel assembly moves along rails on the mainstructure of the gun (to facilitate recoil and to open up the chamber) and there was play in each of these fittings. It is possible, then, that both or either of the alignments of the barrel/recoil assembly reative to the gun's main structure (fixed by the vice), and the gun barrel relative to the assembly, could be altered due to the set of elastic waves generated at each firing. An estimate of the angle shift related to scatter at the target is 10 cm/ 25 m = 0.004 radians. This angle shift of a barrel assemby 10cm in length will be accomplished if the play in the fittings is of order 0.4 mm end-to-end, a not unreasonable amount. Suggestions have been made to the gun manufacturer that firing tests be repeated with the play reduced or eliminated by shims inserted at convenient places.

(c) Since the sugar cubes placed on the barrel jump just after the bullet and exhaust gases have left the barrel, it is appealing to attribute their motion to the response of the barrel to the release of pressure in the barrel.

6. Rifling

Although we did not pursue any analysis with respect to rifling, we include a short description. The grooves inside the barrel seems (Figure 8 provides an example), give the bullet speed and rotation. Since the inside of the barrel is of a smaller diameter than the bullet, when the cartridge is fired, the bullet is forced into the barrel and the rifling engages the bullet, deforming it somewhat. Then, as the bullet is propelled down the barrel, it follows the shape of the interior surface and is forced to spin.

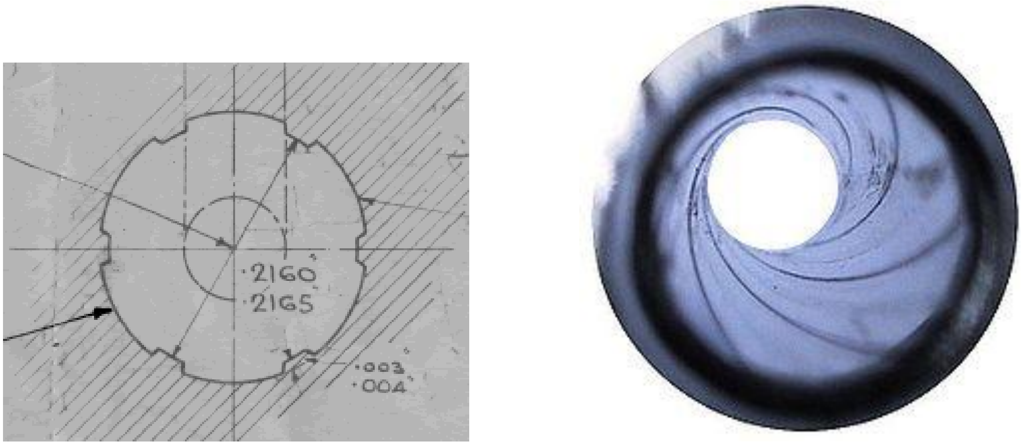

Figure 8. Cross section of the barrel and a view down the barrel.

The grooves used in standard handgun have fairly sharp edges. The sharply edged surface inside of the barrel as seen in Figure 8, only causes friction in the level at approximately 2% of the whole energy. To reduce this friction, and possibly for easier manufacture, there has been interest in other geometries of the grooves. Instead of standard rifling, octagonal rifling has been developed, as it seems to produce better accuracy due to the fact that it does not damage the bullet as badly as conventional rifling. See Figure 9.

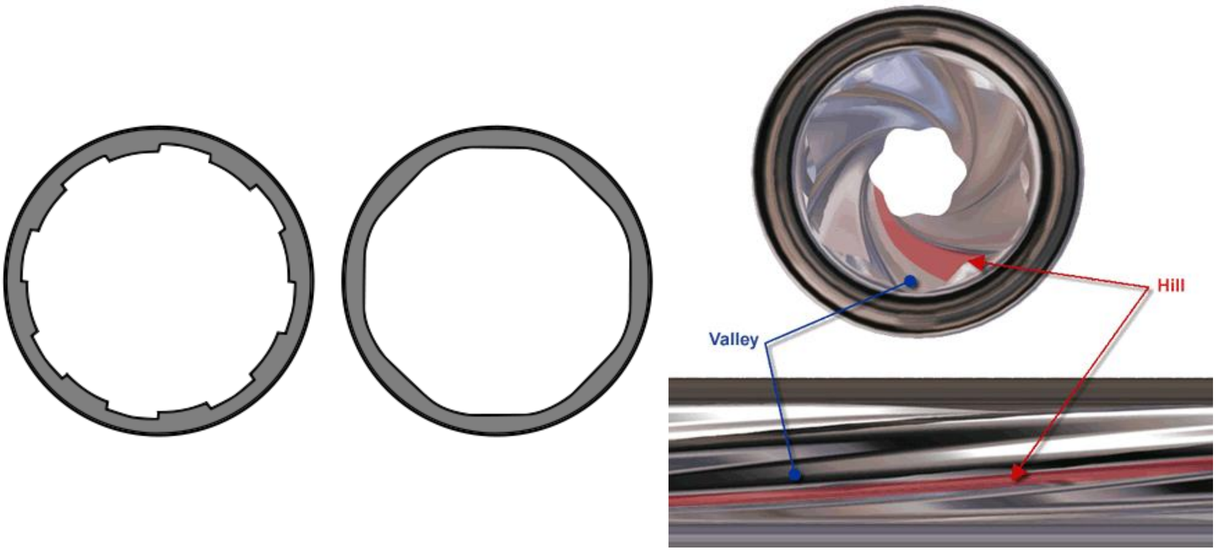

Figure 9. Conventional rifling pattern, polygonal rifling pattern and hammer forged 6-right polygonal rifling pattern

7. Conclusions

Various causes for angle and speed scatter were suggested in Section 3. The analysis presented in Section 4 discounts most of these. The causes remaining consist of bullet variability, and play in the fit of the barrel in its housing and the barrel/ recoil assembly in its slides. There were no available resources to test the former. Slight play in the gun examined and tested was estimated as a possible cause for angle scatter in terms of angle variations due to a misaligned barrel. Speed scatter is harder to attribute to this cause. It has been suggested to the gun manufacturer to repeat the test firings with the play reduced, and to compare results with the previous ones.

8. Acknowledgements

The study group acknowledges the contribution by the problem presenter Murat Alemdaroglu for his efforts through the study group and the organizers of the study group and other contributors of the study group whose names could not be identified.

References

[1] Polygonal rifling, http://en.wikipedia.org/wiki/Polygonal_rifling

[2] Bullet, http://en.wikipedia.org/wiki/Bullet

[3] Rifling Barrel Bullet Grooves Firearm Number Accuracy Propelled, http://www.economicexpert.com/a/Rifling.htm

A Medical Waste Sterilizer

Problem Presenter

Suat Hacısalihoğlu

Chair, Chamber of Commerce and Industry, Trabzon, Turkey

Problem Statement

Sterilization of medical waste is very important for the environment, as the exposition may result in various diseases because of viral or bacterial content of the waste. There are devices developed for this purpose aiming to sterilize the waste in a form called batch process, meaning that a certain amount of waste is placed into the system and subjected to a sterilization procedure for a while and removed from the system afterwards. The procedure is repeated by the next set of waste till the whole set is sterilized.

Our aim, however, is to design a device, a rotating cylinderical container having tubular lights attached to the walls inside, through which the waste is exposed to ultraviolet light as it gets rotated and moved towards the exit. The process will continue till the whole set is fed into the system. Such a device would be more effective as compared to batch processing types. The study group is asked to develop a mathematical model to analyse the effect of the number and location of tubes which will lead to maximal exposure during certain amount of time, which also needs an estimate, the sample will reside in the device before it gets discharged.

Report author

Erhan COŞKUN (Karadeniz Technical University, Trabzon, Turkey)

Contributors

Elif BAŞKAYA, Karadeniz Technical University, Trabzon

Kemel BENTAHAR, (Oxford University, OCCAM)

Olgun CABRI, Artvin Çoruh University

Erhan COŞKUN, Karadeniz Technical University, Trabzon

Ayşe KABATAŞ, Karadeniz Technical University, Trabzon

John OCKENDON (Oxford University, OCCAM)

1. Problem Statement

The company would like to design a device as indicated in Figure 1. Medical waste is to be continuously fed into the device from the top and follow a helical path as it moves down.

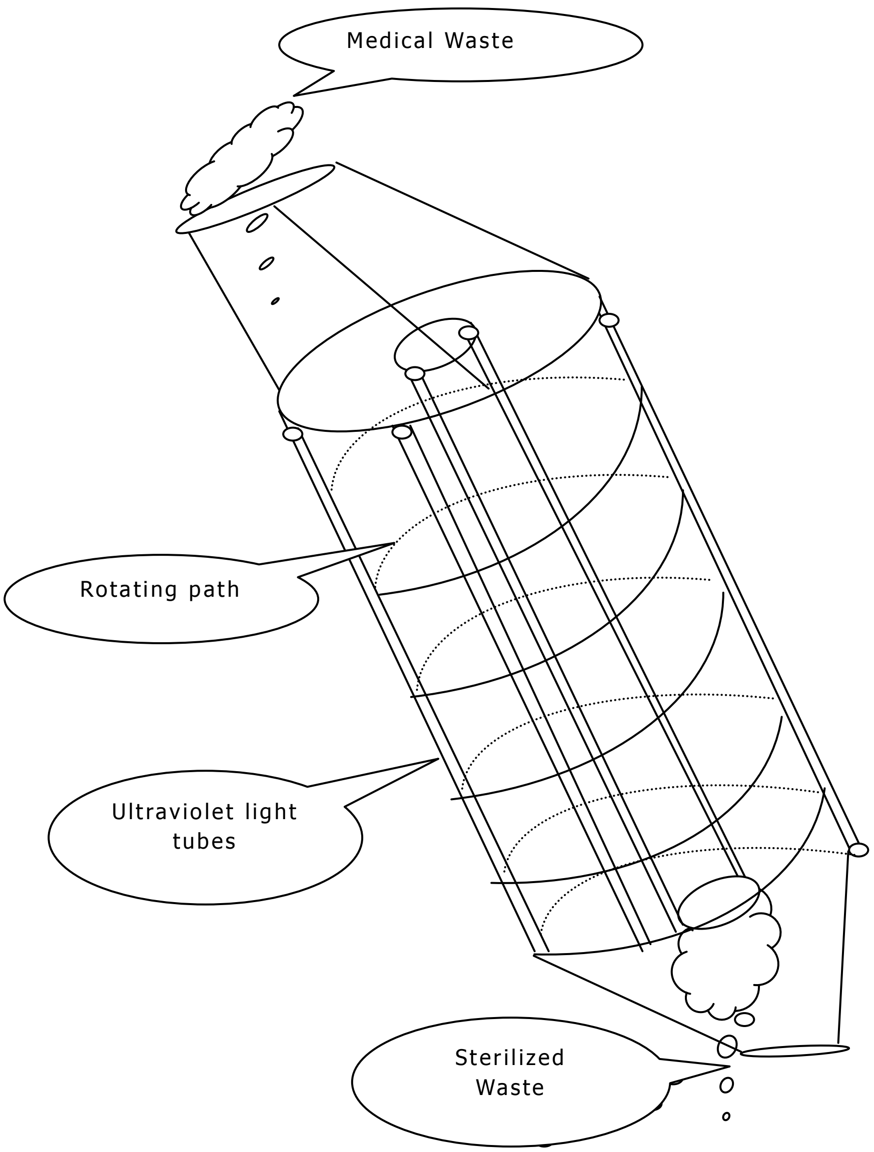

Figure 1: A rotating cylinderical device to sterilize medical waste through ultraviolet light as the waste follow a helical path to the exit.

The path will have all that it needs to allow all the pieces move down simultaneously, without getting stuck somewhere along it's way down to exit. The medical waste will get exposed to ultraviolet light through the tubes along the devices. The tubes remain in their position, while the pieces of waste will rotate around them. Each piece of waste, after having certain exposure to light, will leave the device with hopefully the minimal viral or bacterial content left over.

The company would like to have some scientific guidance concerning the

- number of Ultraviolet(UV) light tubes to be used
- location of the tubes
- exposure time, thus optimal rotational velocity of the device
- effect of having light sources of different magnitudes

which, all together, will hopefully help for a better design.

The study group considered only one dimensional(radial) variations between the inner and outer cylinder, as shown in Figure 2:

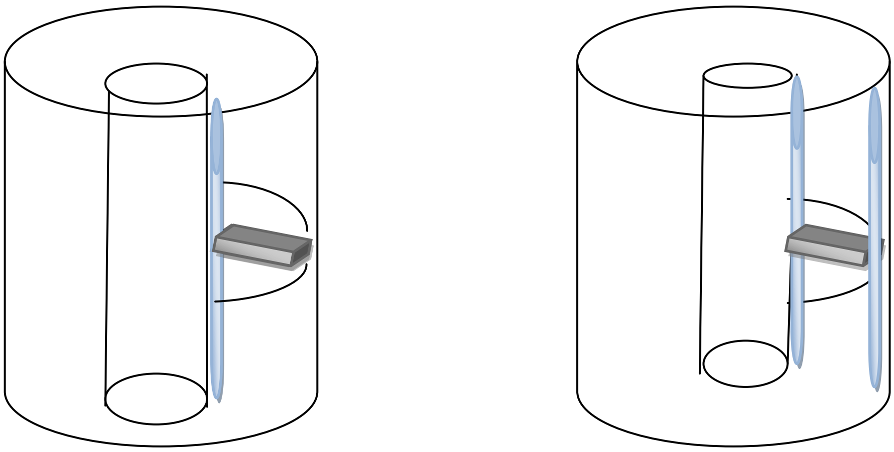

(a) (b)

Figure 2: A piece of medical waste 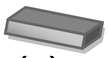 along a path between two cylinders, exposed to sigle (a) and double (b) UV light sources

Two cases are considered: a UV light source from one side(a) and two sides (b) A schematic of an object to be sterilized is shown in Figure 3.

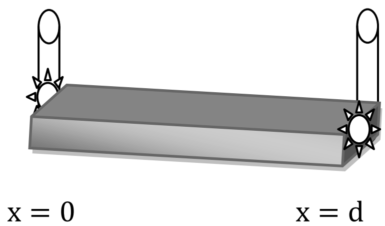

Figure 3: Schematic of an object to be sterilized with UV light sources at each end

Model assumptions:

- We assume that the object has a length d, which is also the distance between the inner and outer cylinder.
- The light source penetrates through the sample and decays exponentially as a function of the distance from the source: For a source located near $x = 0$, we assume that the sample gets exposed to a light source of the form
$$Q(x) = qe^{-kx}, q > 0, k > 0$$
from a light tube near $x = 0$, whereas the tube located near $x = d$, would yield a source
$$Q(d - x)$$
- The rate of decay of medical content(concentration) $c(x, t)$ at point x and time t is proportional to the the existing concentration at that point, with the decay factor $Q(x)$, the strength of ultraviolet light acting on the object at that point.

2. Models and analysis

We consider three cases:

Case I: a single UV light source located along the inner or outer cylinder.

Case II: two light sources located along both inner and outer cylinder near both ends of the object.

Case III: As in case II, but with sources of different magnitudes

Case I Single light source

Therefore, for a single light source we have the simple model

$$\frac{\partial c(x,t)}{\partial t} = -Q(x)c(x,t) \tag{1}$$

with the initial condition

$$c(x, 0) = 1 \tag{2}$$

meaning that the object is initially contaminated hundred percent. The solution to the Cauchy problem is

$$\begin{aligned} c(x,t) &= \exp(-Q(x)t) \\ &= e^{-\left(qe^{-kx}\right)t} \end{aligned} \tag{3}$$

Remarks

- For each fixed $t, c(x,t)$ is an increasing function of x as
$$\frac{\partial c}{\partial x} = kqe^{-kx}e^{-(qe^{-kx})t} > 0$$

This means that more medical content will remain in the object as we examine it further away from the UV light source, which is expected. For $q = 1, k = 1$, and t=0,1,...,10 değerleri için mesh plot of $c(x,t)$ is given in Figure 4

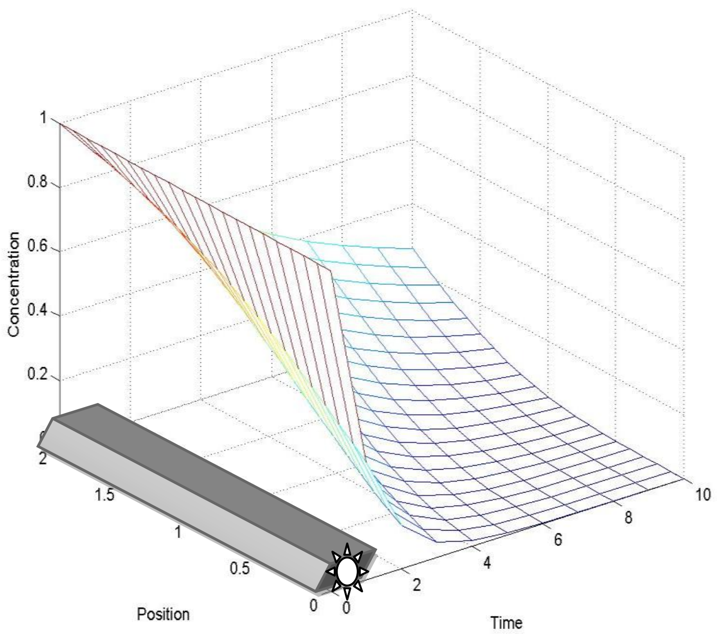

Figure 4: An object(rectangular prizm) under sterilization with a single light source as t increases

- For each value of x, the concentration decreases exponentially as a function of time, with the highest values along the other end, $x = d$.
- For a given $\epsilon > 0$, the time T_1 it takes to have the maximum concentration, the concentration at $x = d$, to be equal to ε can be determined as follows:
$$c(d, T_1) = e^{(-qe^{-kd})T_1} = \epsilon$$
from which we get
$$T_1 = \frac{e^{kd}}{q}\ln(\frac{1}{\epsilon})$$

So we have $c(x,t) < \epsilon$ for all $(x,t), 0 \leq x \leq d, t > T_1$.

Case II: Double light sources of the same magnitude

In this case the decay factor at a point x will be the sum of the light sources $Q(x)$ and $Q(d-x)$. Therefore, we will have

$$\frac{\partial c(x,t)}{\partial t} = -(Q(x) + Q(d-x))c(x,t) \quad (4)$$

with the same initial (2). The solution to (2)-(4) is

$$c(x,t) = e^{-(Q(x)+Q(d-x))t} \quad (5)$$

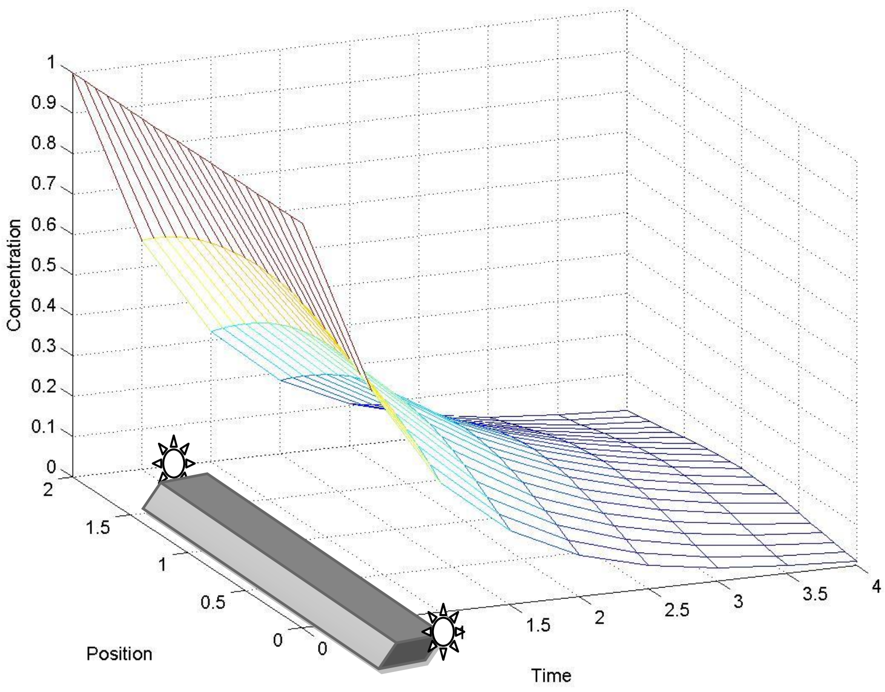

Figure 5: An object(rectangular prizm) under sterilization with two light sources as t increases

Remarks

- For each value of x, the concentration decreases exponentially as a function of time, with the highest values along the middle, $x = \frac{d}{2}$ where $Q(x) + Q(d-x)$ assumes its smallest value.

- For a given $\epsilon > 0$, the time T_2 it takes to have the maximum concentration, the concentration at $x = d/2$, to be equal to ε can be determined as follows:
$$c(d/2, T_2) = e^{-2(Q(d/2)T_2} = \epsilon$$
From which we get
$$T_2 = \frac{e^{kd/2}}{2q} \ln(\frac{1}{\epsilon})$$
So we have $c(x,t) < \epsilon$ for all $(x,t), 0 \le x \le d, t > T_2$.
- The comparison between T_1 and T_2:
we would like to compare the time values to have the maximum concentration become less than a prescribed value ϵ to see the effect of having UV light sources on each side of the cylinder.
$$T_2 = \frac{e^{kd/2}}{2q} \ln\left(\frac{1}{\epsilon}\right) = \frac{1}{2}\sqrt{\frac{\ln(\frac{1}{\epsilon})}{q}}\sqrt{\frac{e^{kd}}{q}\ln(\frac{1}{\epsilon})} = \frac{1}{2}\sqrt{\frac{\ln(\frac{1}{\epsilon})}{q}}\sqrt{T_1} \tag{6}$$
The relation (6) implies that sterilization time with two light sources is proportional to that required by a single light source. So, quite unlike the common sense expectation of the relation $T_2 = \frac{1}{2}T_1$, the advantage of having two sources is considerably high.

- The advantage of having two sources is apparent from the illustrations shown in Figure 4 and 5. The concentration decays slowly and ununiformly with a single light source as shown in Figure 4, whereas the decay is much faster and has a rather uniform nature with two sources of light, as shown in Figure 5.
- Average concentration versus time graphics are illustrated in Figure 6.

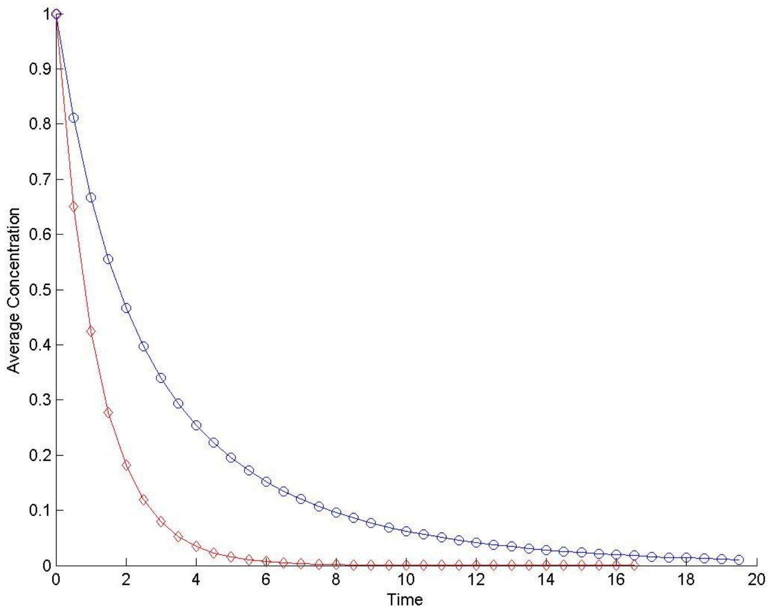

Figure 6: Average concentration versus time:(o) single, (◇red) two light sources

Case III: Double light sources of different magnitudes

In this case we assume that the two light sources with different magnitudes: $Q_1(x) = q_1 e^{-kx}, Q_2(d-x) = q_2 e^{-kx}$

So then we have

$$\frac{\partial c(x,t)}{\partial t} = -(Q_1(x) + Q_2(d-x))c(x,t) \tag{7}$$

with the same initial (2). The solution to (2),(7) is

$$c(x,t) = e^{-\left(Q_1(x)+Q_2(d-x)\right)t} \tag{8}$$

The solution (8) have also the same qualitative behaviour as the previous ones, except that setting $\frac{\partial c}{\partial x} = 0$ we have $x = \frac{d}{2} + \frac{1}{2k}\ln(\frac{q_1}{q_2})$, where $c(x,t)$ assumes its maximum for each t. In this case we have an asymmetric sterilization along the sample. In case $q_1 = q_2$, the maximum point shifts to the center, expectedly.

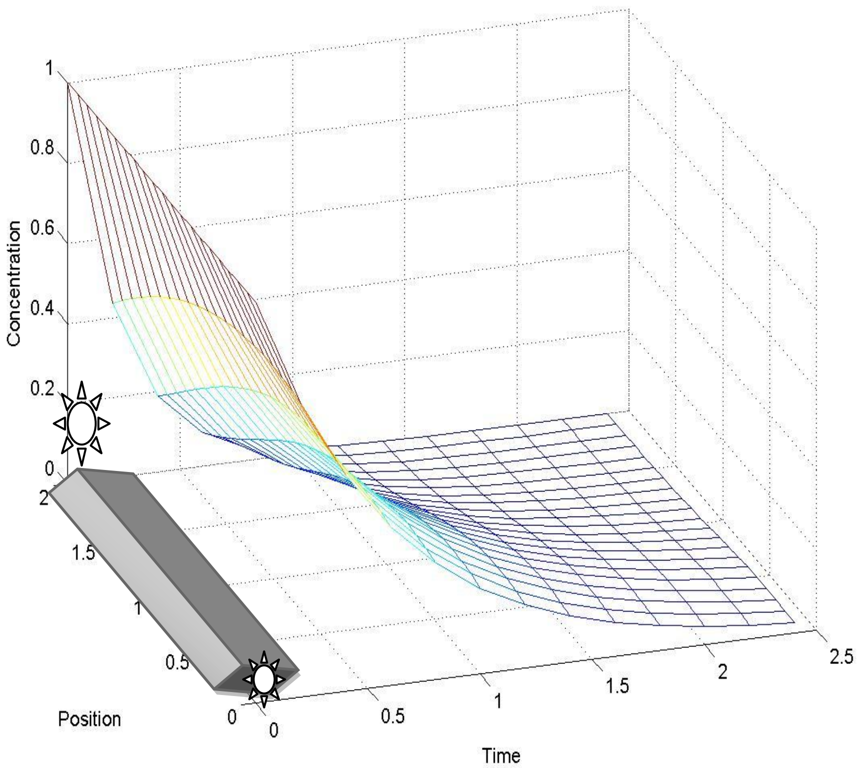

Figure 7: An object(rectangular prizm) under sterilization with two light sources of different magnitude($q_1 = 1, q_2 = 4$) as t increases

Finally we can determine the time it takes to have a concentration less than a prescribed value ϵ.

Similar to the algebra above, we find the required time to be equal to

$$\overline{T_2} = \frac{e^{kd/2}}{2\sqrt{q_1 q_2}} \ln(1/\epsilon) \quad (9)$$

Notice that if $q_1 = q_2$ then we have $T_2 = \overline{T_2}$.

There does not seem to be a practical advantage for using UV lights of different magnitude.

3. Optimal Rotational Velocity

Having determined the time needed to have a concentration less than a prescribed value for each cases, the next question is how to determine the rotational velocity of the device so as to keep the object within the sample for the estimated amount of time.

We will carry out the computations for each Case. But first we look at the first case

Let b the axial distance between the helical curves , L the length of the cylinderical device

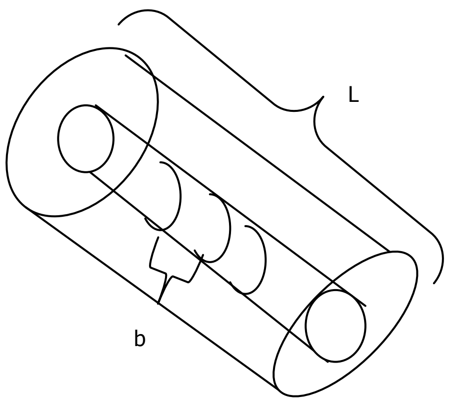

Figure 8: Helical curves around the inner cylinder with radius r

Let ω be the rotational speed of the inner cylinder and v be the downward velocity of the object on the helical path.

Then the time required for a single rotation is $\tau = 2\pi/w$. Since b units of axial distace is travelled during this time, the axial velocity of the object is given by $v = \frac{b}{\tau}$

The time it takes for the object to complete its travel is then given by
$T = \frac{L}{v} = \frac{L\tau}{b} = \frac{2\pi L}{wb}$

which is also the object's residence time in the device. For the required level of sterilization with a single light source, $T \geq T_1$, i.e.,

$$\frac{2\pi L}{wb} \geq \frac{e^{kd}}{q}\ln(\frac{1}{\epsilon})$$

or, $w_1 = w$ will have to satisfy

$$w_1 \leq = \frac{2\pi L}{bT_1} = \frac{2\pi L}{\frac{e^{kd}}{q}\ln(\frac{1}{\epsilon})b}$$

Asuming that one needs to save energy, then optimal rotational speed will be given by

$$w_1(opt) = \frac{2\pi L}{\frac{e^{kd}}{q}\ln(\frac{1}{\epsilon})b} \tag{9}$$

Similarly for case II, we need $T \geq T_2$, so we have

$$w_2 \leq = \frac{2\pi L}{bT_2} = \frac{2\pi L}{\frac{e^{kd/2}}{2q}\ln(\frac{1}{\epsilon})b}$$

Therefore, the optimal rotational speed will be given by

$$w_2(opt) = \frac{2\pi L}{\frac{e^{kd/2}}{2q}\ln(\frac{1}{\epsilon})b} \tag{10}$$

Comparing $w_1(opt)$ and $w_2(opt)$ using the relation

$$\frac{w_1(opt)}{w_2(opt)} = \frac{T_2}{T_1} = \frac{\frac{1}{2}\left(\frac{\ln\left(\frac{1}{\epsilon}\right)}{q}\right)^{\frac{1}{2}}}{\sqrt{T_1}}$$

Or

$$w_2(\text{opt}) = \frac{w_1(\text{opt})\sqrt{T_1}}{\frac{1}{2}\left(\frac{\ln\left(\frac{1}{\epsilon}\right)}{q}\right)^{\frac{1}{2}}}$$

4. Conclusions and recommendations

The simplest as is, the the model reveals many important clues for an effective design of a medical sterilizer.

- We determined the time needed to sterlize a single object up to a given required precision by using single and double light sources along the inner and outer cylinders.
- We determined that the time needed to sterilize an object with light sources along both inner and outer tubes is proportional to the square root of that required by a single light tube. This result, though seem to contradict with common sense, implies considerable saving .
- We determined optimal rotational speeds that will allow the object to remain in the system so a to get sterilized to a give precision. Furthermore, developed a relation between optimal rotational speeds of the device having a single or double light tubes. Adding an extra light tube allowes for a faster rotation.
- Light sources of different magnitudes do not lead to any advantage in terms of sterlization time, other than just the shift in the location of the path for the maximum UV exposure.
- The parameters q, k in the decay factor $Q(x) = qe^{-kx}$ can be estimated for certant type of medical wastes, this, in turn, will effect rotational speed.
- The model assumes a continuous exposure from the light sources, whereas in reality, the object's distance to light source changes as it revolves. So a more realistic model should be developed to take this situation into account.

5. Acknowledgements

The study group acknowledges the contribution by the problem presenter Suat Hacısalihoğlu for his efforts through the study group and the organizers of the study group.

References

[1] Wladyslaw Kowalski, Ultraviolet Germicidal Irradiation Handbook, Springer-Verlag, 2009.

Participants

Faculty

Mehmet AKBAŞ	KTU	akbas@ktu.edu.tr
Fatma Gül AKGÜL	KTU	
Nagehan AKGÜN	ODTU	nalsoy@metu.edu.tr
Ömer AKIN	TOBB ETÜ	omerakin@etu.edu.tr
Murat ALEMDAROĞLU	TİSAŞ	
Rovshan ALİYEV	KTU	
İsmail H. ALTAŞ	KTU	ihaltas@ktu.edu.tr
Mete AVCI	KTU	mavci@ktu.edu.tr
Selçuk Han AYDIN	KTU	shaydin@ktu.edu.tr
Adnan BAKİ	KTU	abaki@ktu.edu.tr
Elif BAŞKAYA	KTU	elifbekar@ktu.edu.tr
Alemdar BAYRAKTAR	KTU	alemdar@ktu.edu.tr
Mustafa BAYRAM	YTU	msbayram.yildiz.edu.tr
Kemal BENTAHAR	OCCAM,Oxford University, UK	bentahar@maths.ox.ac.uk
Murat BEŞENK	KTÜ	mbesenk@ktu.edu.tr
Olgun CABRİ	Artvin Coruh University	olguncabri@artvin.edu.tr
Menşure CAN	KTU	m.can@ktu.edu.tr
Wan CHEN	OCCAM,Oxford University, UK	chenw1@maths.ox.ac.uk
Hamit CİHAN	KTU	
Lale CONA	Gumushane University	lale_cona@hotmail.com
Erhan COŞKUN	KTU	erhan@ktu.edu.tr
Haskız COŞKUN	KTU	haskiz@ktu.edu.tr
Ellis CUMBERBATCH	Claremont Graduate University, USA	ellis.cumberbatch@cgu.edu
İshak CUMHUR	Rize University	ishak.cumhur@hotmail.com
Zafer ÇAKIR	Gumushane University	zafer@gumushane.edu.tr
Abdullah ÇAVUŞ	KTU	cavus@ktu.edu.tr
Necati ÇELİK	Gumushane University	necaticelik1@hotmail.com
Hüsnü Anıl ÇOBAN	KTÜ	h.anil_coban@hotmail.com
Bahadır ÇOR	ODTU	e132683@metu.edu.tr
Alican DALOĞLU	KTU	daloglu@ktu.edu.tr
Mutlu DEDETÜRK	Gumushane University	mtturk@yahoo.com
Ali Hikmet DEĞER	KTÜ	ahikmetd@ktu.edu.tr
Fatma Zehra DOĞRU	KTU	fatmazehradogru@gmail.com
İbrahim DÜZGÜN	Gumushane University	ibrahim-duzgun@hotmail.com
Murat EKİNCİ	KTU	ekinci@ktu.edu.tr
Ahmet GÖKDOĞAN	Gumushane University	ahmet.gokdogan@gmail.com
Nurgül GÖKGÖZ	ODTU	nurgul.gokgoz@gmail.com
Cevat HACIYEV	KTU	haciyev@ktu.edu.tr

Zameddin İSMAİLOV	KTU	ismailov@ktu.edu.tr
Bülent KARASÖZEN	METU	bulent@metu.edu.tr
Ayşe KABATAŞ	KTU	aysekbts@hotmail.com
İsmail KAYA	KTU	ikaya@ktu.edu.tr
Gülay İlona Telsiz KAYAOĞLU	Mimar Sinan Fine Arts University	gtelsiz@msgsu.edu.tr
Temel KAYIKÇIOĞLU	KTU	tkayikci@ktu.edu.tr
Orhan KESEMEN	KTU	okesemen@gmail.com
Tülay KESEMEN	KTU	tkesemen@gmail.com
Tahir KHANİYEV	TOBB ETÜ	tahirkhaniyev@etu.edu.tr
Ali KONURALP	Celal Bayar Üniversitesi	ali.konuralp@bayar.edu.tr
Onur KÖKSOY	Nigde University	okoksoy@nigde.edu.tr
Cemal KÖSE	KTU	ckose@ktu.edu.tr
Nesibe MANAV	Artvin Coruh University	
Nesrin MANAV	Afyon Karahisar University	nesrinmanav2@gmail.com
Mehmet MERDAN	Gumushane University	mmerdan@ktu.edu.tr
Vasıf NABİYEV	KTU	vasif@ktu.edu.tr
John OCKENDON	OCCAM,Oxford University, UK	ock@maths.ox.ac.uk
Halil İbrahim OKUMUŞ	KTU	okumus@ktu.edu.tr
İdris ÖREN	KTÜ	oren@ktu.edu.tr
Fatma Yerlikaya ÖZKURT		fatmayerlikaya@gmail.com
Ömer PEKŞEN	KTU	peksen@ktu.edu.tr
Tim REİS	OCCAM,Oxford University, UK	reis@maths.ox.ac.uk
Ayşe SARIAYDIN	ODTU	saayse@metu.edu.tr
Mustafa Zihni SERDAR	Erişim Computer	
Hasan SOFUOĞLU	KTU	sofuoglu@ktu.edu.tr
Süleyman ŞENGÜL	KTU	ssengul@ktu.edu.tr
Uğur ŞEVİK	KTU	usevik@ktu.edu.tr
Münevver TEZER	ODTU	munt@hetu.edu.tr
Önder TÜRK	ODTU	oturk@metu.edu.tr
George TÜRKİYYAH	American Univ. Lb	
Mustafa ULUTAŞ	KTU	ulutas@ieee.org
Ahmet ÜNAL	KTU	unal@ktu.edu.tr
İhsan ÜNVER	KTU	ihsanunver@ktu.edu.
Yüksel VARDAR	KTU	
Ziya YAPAR	KTU	yaru@ktu.edu.tr
Devran YAZIR	KTU	tkesemen@gmail.com
Students		
Elif Özlem ARDIÇ	KTU	ozzlmm.88@hotmail.com
Merve AYAN	KTU	mervemsi_89@hotmail.com
Selami BAYRAKTAR	KTU	raki_185@hotmail.com
Mehmet CEBECİ	KTU	dejavu_mc@hotmail.com
Ahmet ÇAKMAK	KTU	netscapenetwork@hotmail.com
Yüksel ÇELİK	KTU	karakule_52.7@hotmail.com
Tülin ÇETİN	KTU	cetin_tulin_27@hotmail.com
Reyhan ÇIKRIKÇI	KTU	reyhan-ckrkc@hotmail.com
İbrahim ÇİÇEK	KTÜ	_ibrahimcicek_@windowslive.com
Turgay ÇİFTÇİ	KTU	turgayciftci27@hotmail.com
Seyit DUYAR	KTU	ss.duyar@windowslive.com

Sibel GAN	KTU	sibel_gan87@windowslive.com
Semra GENÇ	KTU	semragenc@hotmail.com
Hüseyin KALKAN	KTU	asi_huseyin61@hotmail.com
İbrahim KİRAZLİ	KTU	math_ibo_kirazli@hotmail.com
Feyza MUTLU	KTU	feyza_fevzi@hotmail.com
Muhsin TAMTÜRK	KTU	samsunlu_1955@hotmail.com
Mehmet Emin TERZİ	KTU	mehmetterzi1985@hotmail.com
Özgür ULAŞ	KTU	ozgur_ulas78@hotmail.com
Neslihan UZUN	KTU	nslyn61@gmail.com
Şeyma UZUN	KTU	seyma_uzun88@hotmail.com
Büşra YILMAZ	KTU	by_088@hotmail.com

A view from opening session, October 4, 2010

Study Group(on the last day!, October 8, 2010)

A panoramic view of Trabzon from University Social Facilities

“The most reliable technological product is the one used, where it is produced” ec.